

6                   **Conceptual model of regional groundwater flow based on**  
7                   **hydrogeochemistry (Montréal Est, Québec, Canada)**

8                   Châtelaine Beaudry<sup>1</sup>, René Lefebvre<sup>1C</sup>, Christine Rivard<sup>2</sup> & Vincent Cloutier<sup>3</sup>

10                  <sup>1</sup> Centre Eau Terre Environnement, Institut national de la recherche scientifique (INRS),  
11                  490 rue de la Couronne, Québec, Québec, Canada G1M 3X3

12                  <sup>C</sup> Corresponding author: 418-654-2651, rene.lefebvre@ete.inrs.ca

13                  <sup>2</sup> Geological Survey of Canada, Natural Resources Canada, Québec, Québec, Canada

14                  <sup>3</sup> Institut de recherche en mines et en environnement (IRME), Université du Québec en  
15                  Abitibi-Témiscamingue (UQAT), Amos, Québec, Canada

17                  ***For the use of the editors***

**Paper #:**

**Submitted on:**

**Accepted on:**

**Application - Research – Commentary – Book Review:**

**Copyright Held by:**

**T2012**

18                  **Abstract:**

19                  [The groundwater geochemistry of the fractured rock aquifer system in the Montréal  
20                  Est region, southern Quebec, Canada, was studied as part of a regional groundwater  
21                  resources assessment. The 9,218 km<sup>2</sup> study area included three major watersheds that  
22                  were divided into five hydrogeological contexts: Northern St. Lawrence Lowlands,  
23                  Southern St. Lawrence Lowlands, Appalachian Uplands, Appalachian Piedmont and  
24                  Monteregian Hills. A large part of this study area was invaded by the Champlain Sea  
25                  from 13,000 to 11,000 years ago. Study objectives were to identify the mechanisms  
26                  controlling groundwater composition and to support the understanding of the aquifer  
27                  hydrodynamics. Groundwater from 206 wells drilled into the rock aquifer was sampled  
28                  and analyzed for conventional parameters and isotopic analyses were also done on  
29                  selected samples ( $\delta^2\text{H}$ ,  $\delta^{18}\text{O}$  and  $^3\text{H}$  of water;  $\delta^{13}\text{C}$  and  $^{14}\text{C}$  of dissolved inorganic

30 carbon). The interpretation of geochemical results was based on a multivariate statistical  
31 analysis, which led to the definition of 8 water groups. The study allowed the delineation  
32 of a 2,200 km<sup>2</sup> zone containing brackish groundwater of marine origin in the north-  
33 western part of the study area. This zone is surrounded by sodic and alkaline groundwater  
34 originating from Na<sup>+</sup>-Ca<sup>2+</sup> ionic exchange. Young groundwater and therefore recharge  
35 zones were only encountered in the southern part of the Lowlands, in the northern part of  
36 the Piedmont and in the Appalachian Uplands. In the southern part of Lowlands, recharge  
37 is presumed to be slow and water composition shows influence of the former presence of  
38 the Champlain Sea. Relatively deep groundwater circulation was also inferred to occur  
39 from the Appalachian Uplands towards mixing zones mainly located to the west at the  
40 Appalachian frontal thrust faults and around Monteregian Hills. The geochemical  
41 interpretation provided indications on regional recharge and discharge zones as well as  
42 groundwater flow, which could not have been determined otherwise.]

#### 43 **Résumé :**

44 [L'étude hydrogéochimique du système aquifère rocheux fracturé de la Montérégie Est,  
45 sud du Québec, Canada, a fait partie d'une évaluation régionale des ressources en eau  
46 souterraine. La région d'étude de 9 218 km<sup>2</sup> couvrait trois bassins versants qui avaient été  
47 divisés en cinq contextes hydrogéologiques : les Basses-terres-du-Saint-Laurent nord, les  
48 Basses-terres-du-Saint-Laurent sud, le Piémont appalachien, les Hautes-terres des  
49 Appalaches, et les Collines montréalaises. Une partie importante de cette région a été  
50 envahie par la Mer de Champlain il y a environ 13 000 à 11 000 ans. L'étude avait  
51 comme objectifs d'identifier les mécanismes contrôlant la composition de l'eau  
52 souterraine et de supporter la compréhension de l'hydrodynamique de l'aquifère. L'étude  
53 est basée sur les analyses chimiques de 206 échantillons d'eau de puits dans l'aquifère  
54 rocheux et d'analyses isotopiques sur une sélection d'échantillons ( $\delta^2\text{H}$ ,  $\delta^{18}\text{O}$  et  $^3\text{H}$  de  
55 l'eau;  $\delta^{13}\text{C}$  et  $^{14}\text{C}$  du carbone inorganique dissous). Huit groupes d'eau ont été définis par  
56 des méthodes statistiques multivariées. L'étude a permis de circonscrire une zone de 2  
57 200 km<sup>2</sup> d'eau saumâtre d'origine marine dans le nord-ouest de la région. Cette zone est  
58 entourée d'eaux alcalines et sodiques résultant de l'échange ionique Na<sup>+</sup>-Ca<sup>2+</sup>. Des eaux  
59 jeunes associées aux zones de recharge sont rencontrées dans le sud des Basses-terres,

60 dans le nord du Piémont ainsi dans les Hautes-terres appalachiennes. La recharge est  
61 présumée lente dans le sud des Basses-terres où la chimie des eaux est influencée par  
62 l'ancienne Mer de Champlain. Une circulation relativement profonde d'eau souterraine  
63 est présumée se produire à partir des Hautes-terres jusqu'à des zones de mélange situées  
64 surtout à l'ouest des chevauchements du front appalachien ainsi qu'autour des  
65 montérégiennes. L'interprétation géochimique a donné des indications clés sur les zones  
66 de recharge et d'émergence de l'eau souterraine et sur le système d'écoulement régional  
67 qui n'auraient pas pu être obtenues autrement.]

68 **Keywords:** hydrogeochemistry, aquifer system, regional flow, conceptual model, marine invasion

## 69 **Introduction**

70 [Montérégie Est is a 9,218 km<sup>2</sup> region located in southern Quebec, Canada, to the east of  
71 Montreal ([Figure 1](#)). The fractured rock regional aquifer system was studied between  
72 2009 and 2013 as part of a systematic aquifer characterization program (PACES)  
73 launched by the province of Quebec in 2008 ([Palmer et al. 2011](#); [MDDELCC 2017](#)).  
74 Besides providing the required PACES outputs, the Montérégie Est study aimed to  
75 develop an efficient integrated approach not only using conventional hydrogeological  
76 techniques and geochemical datasets, but also other information sources, such as  
77 geotechnical soundings, borehole geophysics and surface seismic ([Lefebvre et al. 2011](#);  
78 [Carrier et al. 2013](#)). This approach was adapted from a previously developed  
79 methodology for the characterization of heterogeneity in shallow granular aquifers to  
80 study the migration of contaminant plumes ([Tremblay et al. 2014](#); [Paradis et al. 2014](#)).  
81 For the specific groundwater geochemical study reported in this paper, initial available  
82 geochemical data were sparse and most data were more than 30 years old. There was thus  
83 a need to significantly increase the geochemical dataset to provide a regional  
84 groundwater quality assessment and to help understand the groundwater flow system.

85 Following the example of previous regional aquifer studies ([Cloutier et al. 2008](#);  
86 [Blanchette et al. 2010](#); [Montcoudiol et al. 2015](#); [Pétre et al. 2016](#); [Rey et al. 2017](#)), the  
87 perspective of this work was to use the indications provided by groundwater  
88 geochemistry and isotopes to develop a better understanding of specific aspects of the

89 flow system that could not be determined on the basis of its geological context or by  
90 physical hydrogeological data. Although the processes leading to the geochemical and  
91 isotopic composition of groundwater are identified and graphical evidences of their  
92 occurrence are shown, this work is not meant to explain these processes in details.  
93 Geochemical evidences are rather used to trace the paths of groundwater flow and  
94 identify relationships between different parts of the flow system, from recharge to  
95 discharge areas. The specific objectives of the groundwater geochemical study were thus  
96 to:

- 97 • Define groundwater groups and identify their origins, their relations, and the main  
98 mechanisms controlling their physical and chemical characteristics;
- 99 • Use groundwater groups to support the interpretation of groundwater regional  
100 circulation patterns and identify recharge and discharge zones.]

## 101 **Study Area**

102 [The Montérégie Est region is bordered by the St. Lawrence River to the northwest and by  
103 the states of Vermont and New York (U.S.A.) to the south (**Figure 1**). It covers three  
104 major watersheds: those of the Richelieu River and Missisquoi Bay, which are sub-  
105 watersheds of the Lake Champlain watershed, and that of the Yamaska River. The  
106 territory includes 108 municipalities and ~790,000 inhabitants. Agriculture is one of the  
107 major economic drivers of this region. Five distinct hydrogeological contexts were  
108 defined in Montérégie Est based on physiography and bedrock geology: Northern St.  
109 Lawrence Lowlands, Southern St. Lawrence Lowlands, Appalachian Uplands,  
110 Appalachian Piedmont and Monteregian Hills. **Figure 1** shows the physiographic features  
111 whereas **Figure 2** illustrates subsurface conditions, including bedrock geology and  
112 surficial sediments.

113 **Figure 1. Montérégie Est location and hydrogeological contexts based on**  
114 **physiography. Map also shows topography, main roads, the Champlain Sea**  
115 **maximum marine transgression limit (~13,000 to 11,000 years ago) and the trace of**  
116 **the cross-sections shown on the 3D block diagram of **Figure 2** (dashed red lines).**

117

118 **Figure 2. 3D block diagram of subsurface conditions in Montérégie Est (cross-**  
119 **sections locations shown on Figure 1). The generally east-west cross-section goes**  
120 **from the Lowlands to the Appalachian Uplands and crosses the thrust faults of the**  
121 **Appalachian Front. The generally north-south cross-section remains in the**  
122 **Lowlands but crosses a Monteregian Hill. Till (green) covers most of the bedrock,**  
123 **with local accumulations of fluvio-glacial sediments (orange) or old Quaternary**  
124 **sediments (brown), and is apparent at surface in the Appalachian Piedmont and**  
125 **Uplands. Lacustrine (purple) and marine (light blue) fine sediments can form large**  
126 **accumulations in the North Lowlands (more than 30 m thick).**

127 The St. Lawrence Lowlands occupy the sedimentary St. Lawrence Platform exhibiting a  
128 low deformation and made up of Cambrian and Ordovician black and red shales,  
129 dolostones and limestones (Clark et al. 1979; Globensky 1985). The northern part of the  
130 Lowlands is covered by thick marine clay and silt deposits left by the Champlain Sea.  
131 The maximum extension of the Champlain Sea basin is shown on Figure 1 (Parent and  
132 Occhietti 1988). Occhietti and Richard (2003) corrected the  $^{14}\text{C}$  ages obtained from sea  
133 shells to establish the span of the Champlain Sea between about 13,000 to 11,000 years  
134 before present. Fractured rock aquifers underlying these marine deposits that exceed ~10  
135 m thick contain brackish water. This area of non-potable confined groundwater extends  
136 over ~2,200 km<sup>2</sup> (Beaudry et al. 2011; McCormack 1980), as shown on Figure 3. The  
137 southern part of the Lowlands is covered by variable thicknesses and discontinuous units  
138 of marine clay and till (Gaucher 1984; Prichonnet 1984) causing discontinuous and  
139 variable groundwater confinement contexts (Figure 3).

140 **Figure 3. Confinement level of the Montérégie Est fractured rock aquifer system**  
141 **based on the nature and thickness of overlying sediments and extent of brackish**  
142 **groundwater, to the north of the region.**

143 The Appalachian Uplands correspond to the Internal Humber Zone of the Appalachians,  
144 which are made up of Devonian ridge continental margin rocks highly deformed and  
145 subjected to low-grade metamorphism (Slivitzky and St-Julien 1987; Brisebois and

146 [Nadeau 2003](#)). Maximum elevation is approximately 500 m above sea level. The last  
147 glaciations, from up to 16,000 years ago, eroded the summits and left behind glacial  
148 valleys having a variable thickness of sediments and discontinuous till layers ([Gaucher](#)  
149 [1984](#); [Prichonnet 1984](#)). Groundwater is generally under unconfined conditions in high  
150 elevation and semi-confined down the valleys ([Figure 3](#)). Apart from the northern portion  
151 of the Lowlands, the surficial cover is usually less than 10 m thick, except in valleys. The  
152 Appalachian Piedmont is located in between the Uplands and Lowlands. Its bedrock is  
153 part of the Appalachian External Humber Zone, which is similar to that of the Uplands,  
154 but surface sediments are similar to the southern part of the Lowlands. At the time of the  
155 last glacial maximum, the Piedmont corresponded to the Champlain Sea shore as  
156 illustrated in [Figure 1](#). The fifth hydrogeological context corresponds to Monteregian  
157 Hills, which are seven Cretaceous, mainly mafic, intrusives puncturing the other contexts  
158 along a northwest-southeast axis. Erosion uncovered these plutons and geophysics  
159 revealed the presence of several buried dykes around these hills ([Feininger and Goodacre](#)  
160 [1995](#); [Séjourné et al. 2013](#)). The Champlain Sea level did not reach the summit of most of  
161 the hills.

162 Lands in the Lowlands and Piedmont are widely used for agriculture and also include a  
163 few cities. Monteregian Hills and Uplands are less populated, activities are rural, and the  
164 forest cover is more important. Average annual total precipitation for Montérégie Est is  
165 approximately 1,100 mm/year and average temperature is 5.9 °C, based on 16 weather  
166 stations, for the period from 1970 to 1999 ([Carrier et al. 2013](#)). For the Uplands, the  
167 average precipitation is generally higher and average temperature is generally lower.  
168 Evapotranspiration is relatively constant for the entire region and is equivalent to about  
169 half of total precipitation ([Carrier et al. 2013](#)).

170 Despite the in-depth interpretation of existing and additionally acquired geological and  
171 hydrogeological data (described in [Carrier et al. 2013](#)), several questions remained about  
172 the regional flow system in order to define a more representative conceptual model. The  
173 geochemical and isotopic groundwater data were thus expected to provide information on  
174 the following remaining issues related to the flow system:

- 175 • Even though recharge was estimated using the infiltration model HELP (Schroed-  
176 er et al. 1994; Croteau et al. 2010; Carrier et al. 2013), the location of groundwa-  
177 ter recharge and discharge zones needed to be confirmed through the geochemical  
178 and isotopic signatures respectively associated with young and evolved ground-  
179 waters (Tóth 1999);
- 180 • Although numerical simulations of the flow system have predicted the presence of  
181 nested “Tothian” (Tóth 1963) local, intermediate and regional flow subsystems  
182 (Laurencelle et al. 2013), the hydraulic conductivity of the regional aquifer ap-  
183 peared to exponentially decrease with depth due to fewer open fractures as depth  
184 increases (Laurencelle 2018). There was thus a need for field evidences that could  
185 determine if groundwater flow is restricted to the shallow, more permeable part of  
186 the rock aquifer or rather has a relatively deep regional component. The geochem-  
187 ical signature of groundwater and especially its radiocarbon content were intended  
188 to provide information on groundwater residence time, according to Plummer and  
189 Glynn (2013), Clark (2015) and Han and Plummer (2016);
- 190 • Complementary to the determination of recharge and discharge zones, as well as  
191 the occurrence of regional groundwater flow, there was also a question remaining  
192 about the potential communication between the geological contexts present in the  
193 study area. In particular, it was not known if the presence of the Montereian  
194 granitoids and their associated dyke network has caused a regionally more frac-  
195 tured zone that would have favored long and deep flow paths between the Appa-  
196 lachians Uplands and the adjacent Lowlands;

197 • Finally, the impact of the marine invasion on groundwater outside of the 2,200  
198 km<sup>2</sup> area where brackish groundwater is found in the regional rock aquifer was  
199 unknown. The geochemical characterization was thus also meant to better under-  
200 stand the physical processes involved in the penetration of marine water in the re-  
201 gional rock aquifer and its following long-term leaching by fresh groundwater  
202 ([Laurencelle 2018](#)), as in other areas of the St. Lawrence Lowlands ([Cloutier et al.](#)  
203 [2010](#)).

## 204 **Materials and Methods**

### 205 *Sampled boreholes*

206 [The characterization of groundwater geochemistry and isotopes was carried out through  
207 the sampling of groundwater from boreholes (see next subsection), mostly installed in the  
208 regional fractured rock aquifer that was the focus of the study. Some of the sampled  
209 boreholes were drilled within the framework of the project (and are now integrated to the  
210 observation well network of the Quebec Environment Ministry), but most of the  
211 boreholes were private wells supplying households. All boreholes had a steel casing  
212 across surficial sediments, which was anchored with a casing shoe at the top of the rock  
213 aquifer, and the portion of boreholes through the rock aquifer was open and without  
214 screens. Although the casing of observation wells was sealed through surficial sediments,  
215 this is not generally the case for private wells as the sealing of casings has only become  
216 mandatory in recent years.

217 [Laurencelle \(2018\)](#) and [Carrier et al. \(2013\)](#) provide information about the general  
218 conditions of wells in the study area. Surficial sediment thickness is more important in  
219 the Lowlands (5 to 20 m) compared to the Appalachians (2 to 10 m), which controls the  
220 length of steel casing above the open hole section in the rock aquifer. Static water level is  
221 generally around 5 m below ground and rarely exceeds 10 m. Boreholes are relatively  
222 shallow, being generally less than 50 m deep in the rock aquifer, although boreholes can

223 be deeper in the Appalachians. Hydraulic conductivity ranges from about  $10^{-6}$  m/s in the  
224 shallow part of the rock aquifer to about  $10^{-8}$  m/s at a depth of about 50 m in the rock  
225 aquifer, due to the decrease in the occurrence of open fractures with depth. However,  
226 there is a lot of variability in fracturing and thus in hydraulic properties.

227 [Jackson and Heagle \(2016\)](#) have warned about the limitations of using private wells for  
228 the purpose of assessing baseline groundwater quality in relation with shale gas  
229 exploitation. However, at the regional scale it would be prohibitive to install boreholes  
230 dedicated to the establishment of groundwater geochemistry to obtain an adequate spatial  
231 coverage. [McIntosh et al. \(2014\)](#) have actually shown that the sampling of private wells  
232 could provide very important data about regional groundwater geochemistry. Still, the  
233 implications of using open boreholes to sample groundwater have to be recognized. An  
234 important implication is that groundwater samples represent aggregates of groundwater  
235 coming from different depths in the rock aquifer. The shallow part of the rock aquifer  
236 being more fractured and permeable, it is likely that more active groundwater flow could  
237 take place in that zone where more recently recharged groundwater could be present.  
238 Another implication is that preferential infiltration could take place along the steel casing  
239 and affect the groundwater geochemistry. However, very few wells actually have a  
240 geochemical signature that would indicate anthropic contamination, such as the presence  
241 of nitrate ([Carrier et al. 2013](#); [Beaudry, 2013](#)). Furthermore, results presented in this  
242 paper show groundwater geochemistry that is coherent with the hydrogeological context,  
243 such as the presence of reducing groundwater under confined conditions and radiocarbon  
244 proportions indicative of the dominance of evolved groundwater with a long residence  
245 time. Thus, the nature of sampled wells found in the study area did not preclude the  
246 definition of representative groundwater geochemical conditions.]

#### 247 ***Data Collection***

248 [Groundwater from 206 wells drilled into the regional fractured rock aquifer was sampled  
249 in 2010 and 2011, including 178 private wells and 28 observation wells. Each sample is  
250 representative of the complete water column of the well and was sampled according to a  
251 standard sampling procedure ([Beaudry 2013](#); [Carrier et al. 2013](#)). The analytical program

252 for each sample included physicochemical parameters and major, minor, and traces  
253 inorganic elements such as alkalinity, 30 metals, nutrients and sulfur. Stable isotopes of  
254 water ( $\delta^2\text{H}$  and  $\delta^{18}\text{O}$ ) were analyzed for a subset of 90 samples. Tritium ( $^3\text{H}$ ) and  
255 radiocarbon ( $^{14}\text{C}$ -DIC) were analyzed as indicators of groundwater residence time on 44  
256 and 43 samples, respectively, but 5 of the  $^{14}\text{C}$  analyses were on samples with poor ionic  
257 balance that were not included in the geochemical interpretation (there are 3 more  $^3\text{H}$  and  
258 4 more  $^{14}\text{C}$  analyses than reported by [Beaudry 2013](#)). The selection of samples for  
259 isotopic analyses was based on the aim to cover the different hydrogeological contexts, as  
260 well as on knowledge of the area. After verification of the availability of isotopic  
261 analyses for the water types that are defined later in this paper, the addition of three  $^3\text{H}$   
262 and four  $^{14}\text{C}$  analyses was done to better characterize all water types.

263 Geochemical results were compiled into a database, including the site geographic  
264 location, well ID that refers to the full well description in the hydrogeological database,  
265 and the analytical method used. Concentration of carbonate and bicarbonate ions, TDS,  
266 hardness, and ionic balance (in meq/L) were determined using simple equations in a  
267 spreadsheet ([Beaudry 2013](#)). The ionic balance acceptance limit was fixed at  $\pm 15\%$  for  
268 further use of geochemical results. A total of 19 samples exceeded that limit; they were  
269 therefore rejected at first, then treated separately and considered for the interpretation. All  
270 results reported as “undetected” (below the detection limit imposed by the analytical  
271 method) were replaced by a value corresponding to 50% of the detection limit ([Sanford et  
272 al. 1993](#)).]

### 273 *Data Interpretation Techniques*

274 [A statistical method based on [Cloutier et al. \(2008\)](#) was first used to sort all results due  
275 to the large amount of geochemical data. As suggested by [Güler et al. \(2002\)](#), the  
276 multivariate statistical techniques were combined with graphical hydrogeochemical  
277 interpretation to meet the objectives of the study.

278 Multivariate Statistical Analysis (MSA) can be done with a combination of physical and  
279 chemical parameters. Parameters considered in the present study were selected based on  
280 three criteria:

- 281 • Parameters available for most of the samples;
- 282 • A maximum of 10% of a parameter with undetected concentrations;
- 283 • Independence of parameters (for example, Eh and pe are dependent).

284 The 16 parameters selected were *pH*, *TDS*, *pe*, *HCO<sub>3</sub>*, *NH<sub>4</sub>*, *Ba*, *B*, *Ca*, *Cl*, *Mg*, *Mn*, *K*, *Si*,  
285 *Na*, *S* and *SO<sub>4</sub>*. Then, the selection of samples for the MSA was also based on two types  
286 of criteria:

- 287 • Availability of values for all 16 selected parameters;
- 288 • Acceptability of the ionic balance (within  $\pm 15\%$ ).

289 Results for 190 specific samples from bedrock wells having each 16 specific parameters,  
290 constituted the input file for the MSA (190 x 16 matrix) (available in [Beaudry 2013](#)).

291 Hierarchical Cluster Analysis (HCA) MSA method was initially carried out with  
292 *Statistica 6.1*® ([StatSoft Inc. 2004](#)) to group data into families having common  
293 characteristics ([Davis 1986](#)). To do so, Ward's method was selected as a linkage rule,  
294 with Euclidian distances as similarity measurement as done by [Cloutier et al. \(2008\)](#). This  
295 analysis provides a tree diagram representing the linkage distance between each sample.  
296 This diagram starts with a single cluster including all samples with zero loss of  
297 information. When two clusters are joined, information is lost since differences within a  
298 given cluster are disregarded. A phenon line, determined by visual inspection, is used to  
299 find the right compromise between loss of information and a manageable number of  
300 groups.

301 Then, the Principal Components Analysis (PCA) MSA method was carried out with the  
302 same data matrix. PCA is a statistical method used to observe trends in a multivariate  
303 dataset. It simplifies the understanding of the significance of the 16 parameters by  
304 creating new components (called principal components) that better explain the variability  
305 of the chemical composition between samples ([Davis 1986](#)). PCA also helps identify

306 relationships between water groups. Results of the PCA are presented in terms of loading  
307 values. Only the most significant components were kept for the interpretation. ]

## 308 **Results**

### 309 *Multivariate Statistical Analysis*

310 [At a linkage distance (*phenon line*) of 18, the cluster analysis defined 8 water groups  
311 (Figure 4A). Figure 4B shows that the spatial distribution of these water groups is  
312 generally coherent with the hydrogeological contexts of the region (Figures 1 and 2) and  
313 corresponds well to the area where brackish groundwater is found (Figure 3). The names  
314 assigned to these water groups are related to their geochemistry (Figure 5) and their  
315 spatial distribution, which will be further discussed later (Figure 4B): A1 (light blue), A2  
316 (blue) and A3 (purple) are water groups associated with the Appalachians (Uplands and  
317 Piedmont); M1 (red), M2 (orange) and M3 (yellow) are Montereian and “Mixed” types  
318 of water groups; the CS (light green) water group is close to the original Champlain Sea  
319 water geochemistry; and the LL (green) water group mostly occupies the Southern part of  
320 the Lowlands. Colors assigned to water groups are the same for all graphs presented in  
321 the paper.

322 **Figure 4. Results of multivariate statistical analysis of geochemical parameters. A)**  
323 **Cluster Analysis tree diagram defining the 8 water groups below a phenon line of**  
324 **18. B) Spatial distribution of the 190 samples with colored areas belonging to a**  
325 **water group. C) Values of the 1<sup>st</sup> and 2<sup>nd</sup> components of the Principal Component**  
326 **Analysis for the 190 samples identified with their water group. The names of water**  
327 **groups were assigned on the basis of their spatial distribution (Figure 4B) and their**  
328 **geochemical characteristics (Figure 5): three “Appalachian” groups A1, A2 and A3;**  
329 **a “Southern Lowland” group LL; a “Champlain Sea” group CS; and three “Mixed”**  
330 **or “Montereian” groups M1, M2 and M3.**

331 **Table 1** presents loading values of each parameter for the first 5 components of the PCA.  
332 Components 1 and 2 explain together more than 61% of the variance. The third  
333 component only adds 8% and was therefore neglected as well as subsequent components.

334 The principal component scores for these first two components from each sample  
335 (associated to one of the 8 water groups by a color) are illustrated in [Figure 4C](#). This  
336 graph shows that water groups defined by clustering have distinct and coherent global  
337 geochemical characteristics according to the first two principal components obtained  
338 from PCA.

339 **Table 1. Loadings of the 16 geochemical parameters for the first 5 components (C1**  
340 **through C5) of the Principal Component Analysis (bold values indicate dominant**  
341 **parameters).**

342 As illustrated in [Figure 4C](#), cluster analysis and PCA provide together a first basis for  
343 data interpretation. By considering the important loading values of TDS and other salinity  
344 parameters ([Table 1](#)), the 1<sup>st</sup> component can be interpreted as a combination of both fresh  
345 and saline water. Saline waters have negative 1<sup>st</sup> component values whereas low salinity  
346 water has positive values. The 2<sup>nd</sup> component seems to be associated with hardness  
347 ([Table 1](#)). Negative values of the 2<sup>nd</sup> component correspond to high calcium (Ca) and  
348 magnesium (Mg) concentrations, thus high hardness, whereas high positive values  
349 correspond to sodium (Na) concentrations larger than those of Ca and Mg. This graph  
350 will also be discussed later to support the interpretation of groundwater origins and  
351 geochemical evolutions after further describing the geochemical characteristics of water  
352 groups.]

### 353 *Geochemical Characteristics and Spatial Distribution of Water Groups*

354 [Descriptive statistics were calculated for each of the 8 water groups ([Beaudry 2013](#)). The  
355 complete geochemical data set can be found in electronic format in [Beaudry \(2013\)](#) and  
356 can be accessed online. Several hydrogeochemical graphs distinguishing water groups  
357 were used to illustrate the distinct geochemical natures of water groups and help  
358 understand the mechanisms responsible for the geochemical evolution of groundwater in  
359 the fractured rock aquifer system.

360 Based on the water groups defined by HCA, median geochemical characteristics of water  
361 groups were defined. [Table 2](#) summarizes the median values of physico-chemical

362 properties and component concentrations for the water groups. The median  
363 concentrations, calculated for each major ion, provide an indication of the geochemical  
364 profile of each water group. To help visualize differences between water groups, **Figure 5**  
365 shows the proportions of major ion concentrations on a Piper diagram for each sample  
366 (**Figure 5A**), and the average concentrations of major ions on Stiff diagrams for each  
367 group (**Figure 5B**). The implications of the general geochemical composition of water  
368 groups illustrated by **Figure 5** will also be discussed in this section in relation with the  
369 spatial distribution of each water group represented on **Figure 4B**. The pH and pe will  
370 also be mentioned to better describe the geochemical conditions characterizing water  
371 groups (**Figure 6A**). The extent of water group polygons were defined on the basis of  
372 each of the 190 rock aquifer groundwater samples (location and water group), but also by  
373 considering groundwater flow directions indicated by the potentiometric map ([Carrier et  
374 al. 2013](#)). ]

375 **Table 2. Median values of physico-chemical parameters and component**  
376 **concentrations (mg/L) for the water groups defined in **Figure 4** (geochemical data**  
377 **and water group statistics are available in [Beaudry 2013](#)).**

378

379 **Figure 5. Major ions in groundwater. A) Proportions of major ions for each sample,**  
380 **associated with its water group (color) (defined in **Figure 4**), represented on a Piper**  
381 **diagram. B) Median ionic composition for each water group represented by Stiff**  
382 **diagrams (ions represented and concentration scale shown to the left of diagrams).**  
383 **The order of Stiff diagrams is based on relations between water groups and**  
384 **geochemical evolution paths that will be discussed in the section on Major**  
385 **Geochemical Processes.**

386 *Brackish water groups CS and M3*

387 [The brackish groundwater area, located in the Northern Lowlands, is associated with  
388 water groups CS (Champlain Sea) and M3, which are characterized by significant  
389 concentrations of Na<sup>+</sup> and Cl<sup>-</sup> in areas under confined conditions (**Figure 3**). CS waters

390 are found at the northern extremity of the study area, whereas M3 waters are found in the  
391 southern part and eastern fringe of the brackish groundwater area. The CS group is  
392 dominated by the  $\text{Na}^+$ ,  $\text{Cl}^-$ , and  $\text{SO}_4^{2-}$  ions (Figure 5B; Table 2), and has the highest  
393 concentrations of total dissolved solids (TDS) as well as reducing conditions (Figure 6A).  
394 The M3 group is dominated by  $\text{Na}^+$ ,  $\text{HCO}_3^-$  and  $\text{Cl}^-$  ions (Figure 5B; Table 2) and is less  
395 concentrated in TDS than the CS group, but it is quite alkaline (Figure 6A). M3 has the  
396 highest  $\text{HCO}_3^-$  concentrations of all water types. CS waters show significant  
397 concentrations of Sr, Fe, As, S, B and Mn, in decreasing order of importance relative to  
398 concentrations found in the study area (Table 2). M3 waters have relatively high  
399 concentrations of F, Ba, B and As (Table 2). CS and M3 waters are non-potable.]

400 *Monteregian and mixed water groups (fresh and saline) M1, M2 and LL*

401 [The area containing brackish groundwater is surrounded by water groups M1 and M2  
402 and, further south and east by LL water group in the Southern Lowland and north-  
403 western part of the Piedmont. M1 and M2 waters are found in areas that are confined or  
404 semi-confined, whereas LL waters are found under semi-confined and unconfined  
405 conditions. The M1 group has the most alkaline waters of the study area (Figure 6A) and  
406 is dominated by  $\text{Na}^+$  and  $\text{HCO}_3^-$  ions (Figure 5B; Table 2). M1 waters have extremely  
407 low concentrations of  $\text{Ca}^+$ ,  $\text{Mg}^{2+}$  and  $\text{Mn}^{2+}$ , but have relatively high concentrations of F  
408 and S (Table 2). The M2 group is of Na- $\text{HCO}_3^-$  water type, with very low sulfate  
409 concentrations, but relatively high concentrations of Ba, F, S and Sr (Table 2). The LL  
410 water group has a  $\text{Ca}^{2+}$ - $\text{HCO}_3^-$  water type, which is common for recently recharged  
411 groundwater, as indicated by the relatively low residence time of these waters (discussed  
412 later). LL waters have a relatively high TDS average concentration that is indicative of a  
413 remnant of Champlain Sea water signature. LL waters have relatively high concentrations  
414 of  $\text{SO}_4$ , Fe, Mn, Si and Ba and variable concentrations of Cl (Table 2). The Si  
415 concentration of LL waters are actually the highest of the water groups found in the study  
416 area, which are inferred to be related to a slow water infiltration rate through thick till  
417 deposits.]

418 *Appalachian water groups A1, A3 and A2*

419 [The Appalachian groups (A) have quite distinctive geochemical conditions relative to  
420 other water groups. Group A1 waters are of Ca-HCO<sub>3</sub> water type, which is consistent  
421 with recent recharge and as shown by tritium and <sup>14</sup>C data (discussed later). A1 waters  
422 are found mostly in the south-east of the Appalachian Uplands and in Monteregian Hills  
423 that are mostly under unconfined to semi-confined conditions. The low pH and high pe of  
424 A1 indicate oxidizing and acidic conditions (Figure 6A). Water groups A3 and A2 are  
425 relatively more evolved waters, compared to A1, although A3 is still a Ca-HCO<sub>3</sub> water  
426 type, whereas A2 is a Na-HCO<sub>3</sub> water type. A3 waters are dominant in the Appalachian  
427 Uplands and in the north-east part of the Piedmont, which are under semi-confined or  
428 unconfined conditions. A2 waters have relatively high concentrations of Mn, Fe, S and  
429 As (Table 2). Water group A2 is found mostly at the western fringe of the southern half  
430 of the Piedmont, as well as on Monteregian Hills. A2 waters are mostly found within the  
431 limit of the Champlain Sea maximum transgression (Figure 4B). A2 waters have  
432 relatively high concentrations of F, S, Mn and U (Table 2).]

433

#### 434 **Major Geochemical Processes**

##### 435 *Geochemical Conditions*

436 [Figure 6 presents four geochemical graphs further illustrating the geochemical nature of  
437 water groups and allowing an interpretation of important geochemical processes  
438 occurring in this study area. Figure 6A shows variations of pH (log of hydrogen activity)  
439 and pe (log of electron activity) for all water groups (see also Table 2), which are good  
440 indicators of groundwater conditions and evolution. Figure 6A shows the median values  
441 of pe and pH for each water group, as well as the main range of values (“error bars”  
442 indicate the values of the 25<sup>th</sup> and 75<sup>th</sup> percentiles). Each water group identified in  
443 Montérégie Est shows pe values from mildly to strongly reducing waters (Hounslow  
444 1995). Water groups are positioned in Figure 6A according to the spatial associations of  
445 water groups and their inferred geochemical evolution path based on residence time

446 indicators (discussed in section on Water Origins and Ages) and other further elements  
447 discussed in the present section or the next. The A1 water group shows the most  
448 oxidizing conditions with the highest dissolved oxygen concentration (Table 2), which  
449 are consistent with a typical Ca-HCO<sub>3</sub> recharge water type. On the other hand, the CS  
450 water group has strongly reducing conditions, with the lowest dissolved oxygen  
451 concentration (Table 2).

452 The geochemical processes further discussed here are the mixing of brackish water with  
453 fresher waters, carbonate dissolution and ionic exchanges between Na<sup>+</sup> and Ca<sup>2+</sup> ions.  
454 Since the former presence of the Champlain Sea over the study area exerts an important  
455 control over groundwater geochemistry in Montérégie Est, the origin of groundwater  
456 salinity will first be discussed.]

457 **Figure 6. Geochemical conditions for the water groups found in Montérégie Est. A)**  
458 **Average pe and pH values for the eight water groups. B) Champlain Sea water**  
459 **mixing. C) Carbonate dissolution indicated by a Ca/HCO<sub>3</sub> ratio (in mmol/L) of 1:2**  
460 **(dashed line). D) Evidence of groundwater freshening due to Na-Ca ion exchange.**

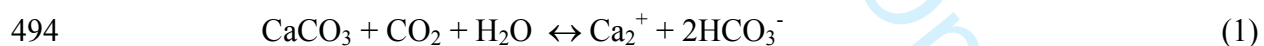
#### 461 *Origin of Groundwater Salinity*

462 [The study area was in large part covered by the Champlain Sea approximately 13,000 to  
463 11,000 years ago (Occhiotti and Richard 2003; see Figure 1 for marine limit). As  
464 demonstrated by Cloutier et al. (2010) for an area located 80 km west of Montérégie Est,  
465 the Champlain Sea water could have invaded the fractured rock aquifer and impart an  
466 important geochemical signature on groundwater. Cloutier et al. (2010) show that the  
467 Champlain Sea water was 34% sea water mixed with 66% of fresh water from melting  
468 glaciers and precipitation. Their calculation was based on the Br/Cl ratio that remained  
469 constant in the sea water, with original concentrations of 0.8385 mmol/L of Br for 535.92  
470 mmol/L of Cl. Based on the numerical modelling of marine water invasion of the rock  
471 aquifer, Laurencelle (2018) suggests that the Champlain Sea may have had a normal  
472 marine water concentration, with dilution occurring in the aquifer rather than the sea.  
473 Figure 6B shows the Br versus Cl concentrations (in mmol/L) for groundwater sampled  
474 in the study area. The black cross represents the global sea water composition (Hem

475 1985), the white circle represents sample S77 found in the Cloutier et al. (2010) study  
476 area that is considered representative of the Champlain Sea water composition after  
477 mixing with fresh water. Samples from water groups CS and M3 plot close to the dashed  
478 dilution line: between Champlain Sea water and fresh water, which means that the  
479 brackish area in the north of Montérégie Est originated from the Champlain Sea invasion.  
480 The CS group composition is similar to the diluted Champlain Sea composition and the  
481 M3 group is further diluted sea water with fresh water. So, the CS water group is  
482 considered as an end-member representing the original composition of brackish  
483 Champlain Sea water in the regional rock aquifer in the areas formerly covered by the sea  
484 (Figure 4). ]

#### 485 *Carbonate Dissolution*

486 [Limestones and dolomites contain Ca and Mg minerals (responsible for the water  
487 hardness) that dissolve relatively easily in groundwater, especially in recharge areas,  
488 where low pH rainwater infiltrates in the aquifer (Appelo and Postma 2005; Clark 2015).  
489 Beaudry (2013) found that saturation indexes of dolomite and calcite (both carbonates)  
490 were especially under-saturated with respect to carbonates for group A1, which means  
491 that if carbonates are present in the aquifer, they will potentially dissolve. Group LL  
492 seems to be more in equilibrium with dolomite and somewhat under-saturated with  
493 respect to calcite. Calcite ( $\text{CaCO}_3$ ) dissolution occurs according to the following reaction:



495 This reaction explains why the type of water associated with recharge is generally  $\text{Ca}^{2+}$ -  
496  $\text{HCO}_3^-$ . Water groups LL and A1 are good examples of the carbonate dissolution  
497 mechanism as shown by the Ca versus  $\text{HCO}_3^-$  graph of Figure 6C. Water groups A3 and  
498 M2 also seem to be affected by calcite dissolution, but with less intensity.

499 The mechanism of carbonate dilution controls Ca and  $\text{HCO}_3^-$  concentrations for water  
500 group A1, while other processes may influence these concentrations for water group LL.  
501 Both groups are located in unconfined to semi-confined conditions in areas contributing  
502 to the regional aquifer recharge (Carrier et al. 2013). Water groups A1 and LL are thus

503 both considered as end-members representing fresh recharge water input into the regional  
504 rock aquifer system, even though LL is also subject to mixing with sea water. ]

### 505 *Freshening / Ion Exchange*

506 [Calcium concentration, relative to sodium, increases due to carbonate dissolution as  
507 discussed previously. On the other hand, sources of sodium are limited to sea water  
508 (characterized by halite dissolution, NaCl), some silicates and a few rarer minerals  
509 (Hounslow, 1995). Water group CS represents sea water with a significant TDS and  
510 sodium (Na) concentrations (Figure 5; Table 2). Water group LL is partly the result of  
511 mixing between fresh water with geologic influence and to a lesser extent sea water.  
512 However, freshening due to Na-Ca ion exchange is responsible for the radical increase of  
513 sodium relative to calcium (Figure 6D), which occurs with a limited increase in TDS  
514 concentration (not shown), especially for water groups M1 and A2.

515 Some of the aquifer materials such as clay minerals (abundant in shales of the Lowlands;  
516 Globensky 1985), organic matter, and metal oxy-hydroxides have the property to sorb  
517 ions (Appelo and Postma 2005; Clark 2015). An adherence is created between cations  
518 and the solid surface of the material. This is called the adsorption phenomenon. Under  
519 steady-state chemical conditions, the exchanger (site of adsorption) is occupied by the  
520 dominant cations. In fresh aquifers,  $\text{Ca}^{2+}$  is often dominant. When sea water infiltrates the  
521 aquifer,  $\text{Na}^+$  becomes a dominant cation and gets adsorbed. When freshening occurred,  
522 after the Champlain Sea had receded,  $\text{Ca}^{2+}$  moved  $\text{Na}^+$  out of the exchanger to get re-  
523 adsorbed. The consequence of this ionic exchange, called freshening, is a rise in the  
524 amount of sodium found in solution, accompanied by a drop in calcium concentration as  
525 shown by Figure 6D. Those Na-rich water groups (M1, M2, M3 and A2) are generally  
526 associated with confined to semi-confined conditions, in bedrock containing clay  
527 minerals, inside the Champlain Sea transgression limit (Figure 4B). The M1 group has  
528 the highest freshening level and, although it is not an end-member representing a  
529 provenance of groundwater, it represents the ultimate state of groundwater evolution due  
530 to Na-Ca ion exchange.

531 Na-Ca ion exchange occurs during the flushing by newly recharged fresh water into parts  
532 of the aquifer system that were formerly invaded by high salinity marine water (Na-Cl  
533 water type). Thus, the freshening process at the origin of Na-Ca ion exchange also  
534 involves the mixing of fresh Ca-HCO<sub>3</sub> recharge water with Na-Cl water having a high  
535 salinity. It follows that the sum of cations in groundwater that has undergone these  
536 combined processes has a higher sum of cations (ultimately only Na) than the sum of  
537 cations that were present dominantly as Ca in the fresh recharge water, even though that  
538 water has an increased concentration in Ca as it evolves and further dissolves calcite  
539 along its flow path. This is seen by the larger concentration of Na relative to Ca in **Figure**  
540 **6D**. When comparing water group A3 that evolves into water group A2, which is  
541 subjected to Na-Ca ion exchange, the sum of Ca and Na ions stays relatively constant  
542 between 2 and 5 meq/L. However, when Na becomes the dominant cation and shows sign  
543 of mixing with marine water (higher Cl), then the sum of cations increases.]

#### 544 *Mixing and Relations Between Water Groups*

545 [Figure 7A shows again samples from water groups relative to the 1<sup>st</sup> and 2<sup>nd</sup> components  
546 of the PCA. This graph is used here to illustrate mixing and geochemical evolution  
547 between water groups. This graph also identifies the inferred groundwater end-members  
548 recognized in the study area, as suggested by Valder et al. (2012).

549 **Figure 7. Mixing and relations between water groups and groundwater geochemical**  
550 **end-members. A) Samples of water groups defined in Figures 4 and 5 according to**  
551 **the 1<sup>st</sup> and 2<sup>nd</sup> components of the Principal Component Analysis (PCA). B) Relative**  
552 **concentrations of major cations (X-axis) and major anions (Y-axis), similar to a**  
553 **Piper plot, supporting relations shown on the PCA graph. Inferred geochemical**  
554 **end-members are superposed on both graphs: Sea Water, Lowland Recharge,**  
555 **Monteregian Water and Appalachian Recharge. These end-members are positioned**  
556 **at the limits of principal components (7A) or ion ratios (7B) representing the general**  
557 **range of end-member values.**

558 By associating the first component of **Figure 7A** with salinity and TDS, the mixing  
559 process can be described. TDS, or salinity, decreases from the left side of the graph to the

560 right: between brackish compositions of the CS end-member (Champlain Sea water), to  
561 the fresh water of the A1 end-member (recharge in the Appalachians). The A1 group is  
562 characterized by the lowest TDS concentrations among water groups. The LL end-  
563 member is found between the A1 and the CS groups. The LL water group features similar  
564 characteristics as A1 (recharge water with low pH and calcite dissolution mechanism),  
565 but with a much higher TDS, representative of diluted sea water. The mixing with  
566 residual Champlain Sea water (which is still potentially trapped in the rock aquifer and  
567 overlying till) and the presumed slow flow where topography is nearly flat, could explain  
568 the high TDS concentrations of the LL group that still bears the geochemical signature of  
569 the Champlain Sea water.

570 The same reasoning can be applied to major ions shown in **Figure 7B**. Similar to the  
571 traditional Piper diagram, the X-axis shows relative concentrations in major cations and  
572 the Y-axis shows the relative concentrations of major anions (in percent and calculated in  
573 meq/L). Three circles (with a continuous line) identify the 3 end-members, A1, LL, and  
574 CS. Based on the ionic composition of these groups, the LL water group plots between  
575 the two others, supporting the mixing hypothesis introduced earlier, although the fact that  
576 LL represents recently recharged water makes it also an end-member.

577 The 2<sup>nd</sup> component of PCA of **Figure 7A** has been associated to hardness. The figure  
578 shows how M1 (red), M2 (orange), M3 (yellow), and A2 (dark blue) groups have  
579 important differences in their hardness, which have been related to a freshening  
580 mechanisms compared to other groups. The M1 group is associated with the highest level  
581 of Ca-Na ion exchange; it is identified as a water evolution end-member, with a dashed-  
582 line circle. The freshening is also clearly identified in **Figure 7B** where sodium-rich  
583 waters are found in the top left corner of the graph. Based on the fact that the highest  
584 concentration of sulfates and chlorides are associated with the CS water type, we can  
585 presume that vertical variations on that graph are mainly explained by its mixture with  
586 sea water (brackish or residual).

587 Therefore, water group M3 is probably a mixture, or an overlap of groups M1 and CS.  
588 For the same reasons, M2 is probably a mixture of groups M1 and LL. Geographically,

589 such mixing makes sense. Due to the geographic distance between A2 and M1, A2 is not  
590 a mixture between A1 and M1. These relations will later be reviewed in the conceptual  
591 model section. ]

592

## 593 **Water Origins and Age**

### 594 *Water Origins*

595 [As a part of the water cycle, groundwater can be characterized according to its isotopic  
596 composition ( $\delta^2\text{H}$  and  $\delta^{18}\text{O}$ ) (Clark and Fritz 1997). A comparison with local meteoric  
597 water lines (LMWL) can help understand water origin in terms of climate or altitude. The  
598 most representative LMWL found for Montérégie Est is the one defined by Cloutier et al.  
599 (2006) for the Basses-Laurentides region, located some 80 km to the west and with  
600 similar elevations?. The Basses-Laurentides meteoric water line (BLMWL) and isotopic  
601 composition of samples from the eight water groups of Montérégie Est are displayed in  
602 **Figure 8A**.

603 Based on the previously mentioned two third dilution hypothesis of the Champlain Sea  
604 water (Cloutier et al. 2010), it is expected that the CS water group will be a mixture of  
605 low isotope fractionation water (sea water; VSMOW of  $\delta^2\text{H}=0\text{‰}$  and  $\delta^{18}\text{O}=0\text{‰}$ ) and  
606 high isotope fractionation water (melting glaciers and precipitation at high latitude).  
607 According to **Figure 8A**, the CS water group, as well as the Lowlands-related water  
608 groups M2, M3 and LL, plot near the top of the graph, with the lowest isotopic  $\delta^2\text{H}$  and  
609  $\delta^{18}\text{O}$  fractionation. On the other hand, water groups associated with topographic highs  
610 (Monteregian Hills, Piedmont and Uplands), plot on the lower part of the graph, which is  
611 representative of a recharge under colder conditions or at high altitude. The M1 water  
612 group plots together with A1 to A3 water groups, which would support the hypothesis  
613 that the M1 water group originates from mixing between fresh water recharged in the  
614 Uplands and saline water from the Lowlands.]

615 *Groundwater Age*

616 [Isotopic indicators of residence time can also help infer groundwater origin and  
617 evolution of the water groups found in Montérégie Est and their interrelations. Tritium  
618 and radiocarbon can provide such indications of groundwater residence time, respectively  
619 for young water (less than about 50 years for tritium) and older water (up to 50 000 years  
620 for  $^{14}\text{C}$ ) (Clark and Fritz 1997). Overall, 42 samples were analyzed for tritium and 43 for  
621 radiocarbon, with 28 samples having both analyses. Figure 8B relates tritium and  
622 uncorrected radiocarbon ages. Samples analyzed for only one of those two parameters are  
623 also represented, in the left and bottom margins of the graph. Ranges of values obtained  
624 for tritium and radiocarbon data for each water group are provided in Table 3.

625 **Figure 8. Isotopic composition of groundwater. A) Stable isotopes of groundwater**  
626 **by groups compared to the Basses-Laurentides meteoric water line (BLMWL;**  
627 **Cloutier et al. 2006). B) Residence time of water groups indicated by tritium ( $^3\text{H}$  is**  
628 **in tritium units, TU) and radiocarbon (non-corrected  $^{14}\text{C}$  ages in years before**  
629 **present, BP). Samples analyzed for only one of the two parameters are represented**  
630 **in the left and bottom margins of the graph. Ellipses indicate the distribution of**  
631 **samples for water groups.**

632 In order to have a better indication of the residence time that is representative of the  
633 different water groups, radiocarbon data were interpreted according to the guidelines  
634 provided by Han and Plummer (2016) and made use of the graphs proposed by Han et al.  
635 (2012). Calculations of corrected radiocarbon ages were done using the interpretation  
636 spreadsheet developed by Janos (2017). Basically this approach identifies the processes  
637 affecting radiocarbon and uses the correction method suitable for these processes. The  
638 interpretation graphs used for the correction of radiocarbon ages and results are  
639 documented in a new appendix added to the thesis of Beaudry (2013), which is accessible  
640 online. Table 3 summarizes the range of corrected  $^{14}\text{C}$  residence times that were obtained  
641 for all water groups, which are illustrated later in Figure 9B. Vautour et al. (2015) found  
642 similar ranges of groundwater residence times in another area of the St. Lawrence

643 Lowlands, although the maximum ages were not as high in their study area, which did  
644 not include remnants of Champlain Sea water.

645 **Table 3. Ranges of tritium ( $^3\text{H}$ ), uncorrected (lab.) and corrected  $^{14}\text{C}$  ages for the**  
646 **water groups.**

647 Water groups LL and A1 have a  $\text{Ca-HCO}_3$  water type that can be indicative of non-  
648 evolved recent recharge groundwater (Clark and Fritz 1997; Cloutier et al. 2010). Data  
649 from these water types plot on the top-left corner of the graph in Figure 8B, with over 10  
650 tritium units (TU), uncorrected  $^{14}\text{C}$  ages under 4000 years before present and corrected  
651  $^{14}\text{C}$  ages corresponding mostly to modern water (Table 3), which confirm they are young  
652 groundwaters in recharge areas or that have had relatively short duration flow paths from  
653 recharge areas. Both water groups show evidence of carbonate dissolution in an open  
654  $\text{CO}_2$  system (appendix of Beaudry 2013), which is compatible with indications provided  
655 by Figure 6C and the undersaturated conditions relative to calcite and dolomite (appendix  
656 of Beaudry 2013), especially for water group A1.

657 At the other end of the age spectrum, Champlain Sea water group CS indicates 2 results  
658 (radiocarbon only) of either uncorrected or corrected  $^{14}\text{C}$  ages around 14,000 years,  
659 which are quite consistent with the Champlain Sea period (13 to 11 ky BP; Occhietti and  
660 Richard 2003; Laurencelle 2018). Intermediate tritium and  $^{14}\text{C}$  ages for water groups M2,  
661 A3, M1 and A2 indicate the importance of young and old water mixing affecting the  
662 residence time of these water groups, which allowed them to evolve geochemically.  
663 Overall, Table 3 shows that the residence time increases from A1 to A3 and A2, which  
664 would lead to more evolved waters. The increase in residence time from LL to M2, to M3  
665 and to CS (Table 3) is consistent with groundwater evolution and mixing with old  
666 Champlain Sea water. Corrected  $^{14}\text{C}$  ages for water group M1 have the largest change  
667 compared to uncorrected ages due to carbonate dissolution associated with Na-Ca ion  
668 exchange (Clark 2015). This process also affected the  $^{14}\text{C}$  ages of water group A3 to  
669 some extent. Water groups A2 and A3  $^{14}\text{C}$  ages were affected by calcite precipitation,  
670 which is consistent with their  $\text{pCO}_2$ -pH relationship and their saturation indexes relative  
671 to calcite (appendix of Beaudry 2013).

672 The M1 water group is somewhat puzzling since it has relatively long residence times,  
673 despite the presence of tritium showing some mixing with young groundwater. The M1  
674 water group is mostly located near Monteregian Hills, which are presumed to represent  
675 preferential recharge areas. A source of old groundwater that can only be from great  
676 depth or long travel paths is thus needed to lead to such evolved groundwater among a  
677 preferential recharge zone. [Pinti et al. \(2013\)](#) found larger helium in groundwater in the  
678 Montérégie Est region compared to other parts of the St. Lawrence Lowlands between  
679 Quebec City and Montreal. Such helium concentrations could represent a preferential  
680 migration path from the Precambrian bedrock, which could perhaps result from the effect  
681 of a large mafic dyke network associated with Monteregian Hills that are found over a  
682 large part of Montérégie Est ([Séjourné et al. 2013](#)).]

### 683 ***Geochemical evolution and residence time***

684 [Even though the geochemical evolution ([Figures 6 and 7](#)) and residence time ([Figures](#)  
685 [8B](#)) of water groups have been discussed successively, the intent is here to briefly wrap  
686 up the description of water groups by combining these two concepts. For that purpose,  
687 [Figure 9](#) shows one indicator of geochemical evolution (Na/Ca in [Figure 9A](#)) versus the  
688  $^{14}\text{C}$  uncorrected age (in order to show data from water groups LL and A1 that have  
689 modern waters), which provides an indication of groundwater residence time. [Figure 9B](#)  
690 graphically shows the corrected  $^{14}\text{C}$  ages for each water groups to demonstrate that the  
691 geochemical evolution illustrated in [Figure 9A](#) is quite coherent with the range of  
692 residence times of the water groups. [Figure 9A](#) clearly shows that geochemical evolution  
693 paths are distinct in the Lowlands and Appalachians, as the geochemical indicators are  
694 quite different for the two domains. Also, [Figures 9A and 9B](#) show together that the level  
695 of geochemical evolution stems directly from the groundwater residence time. Although  
696 water groups are statistically different, there is a continuous evolution of groundwater  
697 through time (as well as through space as shown by the distribution of water types in the  
698 study area in [Figure 4B](#)). For instance, water groups A1, characteristic of recharge zones,  
699 leads to older waters of group A3 found within the Appalachians, and then older and  
700 more evolved still group A2 water, which is found in the Piedmont at the western edge of  
701 the Appalachians. A similar, but not as clear, groundwater evolution path may relate

702 recharge water represented by Lowlands LL water group with the M2 and M1 water  
703 groups. Actually, the evolution path related to these water types are clearer in **Figure 7**,  
704 which may indicate that water group M1 could be related as well to the Appalachian  
705 groundwater evolution path as to the Lowlands evolution path. The relationships between  
706 water groups and the implications of groundwater evolution paths are integrated in a  
707 conceptual model of groundwater geochemical evolution in the next section.]

708 **Figure 9. Geochemical evolution paths and residence time. A) Na/Ca ratio versus**  
709 **uncorrected  $^{14}\text{C}$  ages. B) Corrected  $^{14}\text{C}$  age range of water groups (Table 3). Sample**  
710 **colors are related to water groups as defined in Figures 4A and 5.**

### 711 **Conceptual Model and Discussion**

712 [The integration of all available geochemical data and their interpretation provided the  
713 basis for the development of a conceptual model of regional groundwater geochemical  
714 evolution in the study area. **Figure 10** summarizes the relations between all water groups  
715 and represents the main mechanisms responsible for groundwater evolution.

716 **Figure 10. Conceptual model of groundwater geochemical evolution in Montérégie**  
717 **Est. Each of the 8 water groups is represented with the direction of evolution**  
718 **(arrows), the main mechanisms involved (mixing, geological influence, ion exchange)**  
719 **and the corrected radiocarbon age range (see Table 3).**

720 **Figure 11** is a schematic representation of the Montérégie Est regional flow system based  
721 on the hydrogeochemical interpretation made in the present study. The cross-section  
722 starts from the Appalachian Uplands, to the east, goes through the Rougemont  
723 Monteregian Hill, and then branches northward through the brackish groundwater zone,  
724 towards the St. Lawrence River. Black arrows show groundwater flow directions. The  
725 remainder of this section further describes the geochemical conceptual model and its  
726 implications on the functioning of the regional aquifer system.

727 **Figure 11. Geochemical conceptual model represented by a schematic cross-section**  
728 **from the Appalachian Uplands to the St. Lawrence River. Water group locations**

729 **are illustrated with associated colors and flow directions are represented by arrows.**  
730 **The limit of the former Champlain Sea is indicated by dashed lines on the map and**  
731 **section.**

732 *Champlain Sea invasion area (Water groups CS, M1, M2, M3, LL and A2)*

733 The area of the aquifer system at lower altitude is still affected by the Champlain Sea  
734 invasion (Northern and Southern Lowlands, Piedmont; **Figures 1 and 11**) and by slower  
735 groundwater flow due to the generally flat topography. This area also has low aquifer  
736 recharge (**Carrier et al. 2013**), especially in the northern part of the Lowlands under  
737 confined conditions due to the relatively thick marine clay and silt cover (**Figure 3**).  
738 Furthermore, important groundwater discharge seems to occur at the western edge of the  
739 Piedmont, either due to a topographic effect or the presence of the thrust fault zone, so  
740 the low-lying area further west or north-west does not receive a major contribution of  
741 groundwater originating from the Uplands. The rock aquifer in the area within the limit  
742 of the former Champlain Sea contains either brackish groundwater, which is well  
743 preserved under confined conditions (CS water group) or water with traces of marine  
744 influence under semi-confined to unconfined conditions (LL water group).

745 Groundwater within that area is also characterized by important concentrations of sodium  
746 (and other residual marine components) in solution or adsorbed by the clay minerals of  
747 the rock aquifer made up in large part of shales and mudstones. Groundwater freshening  
748 occurs when fresh water mixes with brackish water in aquifers containing clay minerals  
749 (water groups M1 and A2, see section “Geochemical Conditions”). When bedrock does  
750 not contain clay minerals, or when freshening has already been completed, the mixing of  
751 trapped or residual brackish water with fresh water occurs more as a simple dilution (LL  
752 water group). Water groups M2 and M3 represent transition (or mixing) between those  
753 three contexts, as also supported by  $^{14}\text{C}$  ages (**Table 3**): well preserved brackish water  
754 (CS with original Champlain Sea age; **Table 3**), freshening contexts (M1 and A2) and  
755 brackish water simply diluted by the local recharge of fresh water with geologic influence  
756 (LL). The local recharge is easily identified by young (modern  $^{14}\text{C}$ ; **Table 3**) and fresh  
757  $\text{Ca-HCO}_3$  water, with relatively low pH and with a composition controlled by carbonate

758 dissolution (LL). However, according to the geochemical characteristics, the LL water  
759 group does not seem to be the fresh water source responsible for the water freshening  
760 mechanism. The fresh water origin will be discussed next.

761 *High altitude areas (Water groups A1 and A3)*

762 High altitude recharge is affected by geologic influence, which is not overshadowed by  
763 the high TDS concentrations of sea water as in the low altitude recharge areas. The  
764 physiographic contexts associated with high altitude recharge are the Appalachian  
765 Uplands (mainly south-east), the eastern and southern parts of the Piedmont and some of  
766 the Monteregian Hills. This recharge water is associated with the presence of tritium  
767 (typical of young water; [Table 3](#)), a Ca-HCO<sub>3</sub> water-type with relatively low pH and with  
768 a composition controlled by carbonate dissolution (A1). For water group A1, it is  
769 presumed that total dissolved solids slightly increase due to the relatively fast flow under  
770 unconfined to semi-confined conditions and the high topographic relief. On the other  
771 hand, A3 water group, which is more evolved and corresponds to longer residence time  
772 water ([Table 3](#)), with higher TDS, is dominant in the Upland and the north-east of the  
773 Piedmont, under semi-confined conditions as well as under unconfined conditions. As  
774 expected, the TDS increase is caused by the dissolution of common minerals, generating  
775 a moderate increase in the concentrations of major ion ([Gibbs 1970](#)). pH is also  
776 increasing along flow paths, accompanied by the decrease of dissolved oxygen and pe  
777 ([Figure 6A](#)). Two assumptions still remain to be verified relative to the origin of the A3  
778 water group, considering the relatively long residence time of that group as indicated by  
779 <sup>14</sup>C data ([Table 3](#)):

- 780 1. The presence of a long and relatively deep flow path in the Appalachians,  
781 originating in part from the A1 water group, would lead to the evolution of the A3  
782 water group having a long residence time, or either ;
- 783 2. The A3 water group represents the mixing between modern water with evolved  
784 groundwater from another source (e.g. continuous upward release of groundwater  
785 related to recharge at large depth of ice melting water from the last glaciation).

786 *Hydraulic link between high altitude and Champlain Sea areas*

787 The link between the high and low altitude systems, or the fresh water contribution, is  
788 presumed to be made by the A2 and the M1 water groups, which, as discussed  
789 previously, probably originate from high altitude zones. A2 water group would originate  
790 from the A3 water group, which discharges in the Appalachian Piedmont into the former  
791 Champlain Sea environment. M1 water group would originate in part from high altitude  
792 recharge in the adjacent Montereian Hills. A2 water group is observed in the Piedmont,  
793 whereas M1 water group is locally present in the Southern Lowlands and especially  
794 around some Montereian Hills. The confluence of fresh water (A3) with the former  
795 Champlain Sea environment involves ionic exchange mechanisms. The resulting water  
796 type is characterized by an alkaline Na-HCO<sub>3</sub> water-type, with high sodium  
797 concentrations and low calcium concentrations. The A2 water type is associated with a  
798 lower level of ionic exchange and the M1 water type represents the highest level of  
799 effects from ionic exchange which makes the M1 water type appear as an end-member  
800 among water groups (Figures 7A and 7B).

801 Overall, the groundwater composition in Montérégie Est is largely related to the  
802 hydrogeologic conditions (confined, semi-confined or unconfined) and to the Champlain  
803 Sea influence (associated with topographic lows). This conceptual model of the  
804 groundwater flow system (Figure 11) led to a revision of the initial conceptual model  
805 based on hydrogeological data alone. For instance, the Piedmont is not a preferential  
806 recharge area, as presumed initially at the onset of the project, but rather a discharge area  
807 for deep Appalachian groundwater. Also, in the Appalachian Uplands, due to relatively  
808 low hydraulic conductivity and the limited depth of natural fracturing, it was initially  
809 presumed that groundwater flow would be of a limited vertical extent and therefore  
810 strictly associated to young recharge groundwater, but on the contrary geochemical data  
811 showed that relatively evolved groundwater with long residence times are found in the  
812 uplands (A3), even though the origin of this water is not yet fully understood.

813 The residence time (evaluated with tritium and <sup>14</sup>C ages) increases from A1 to A3 and  
814 A2 (Figures 8B and 9B, Table 3), which would lead to more evolved waters. The

815 increase in residence time from LL to M2, to M3 and to CS (Figures 8B and 9B, Table 3)  
816 is consistent with groundwater evolution and mixing with old Champlain Sea water. The  
817 M1 water group has relatively long residence times, despite the presence of tritium  
818 showing some mixing with young groundwater. An uncertainty still remains about the  
819 actual origin of the M1 water group and the reason for its long residence time despite its  
820 location near some preferential recharge areas of the Monteregian Hills. One potential  
821 hypothesis is that deep waters upflowing along fractured Monteregian dykes could  
822 impart the long  $^{14}\text{C}$  residence times to this water type, even though the presence of  
823 tritium also shows the contribution of recent recharge to this water type. As mentioned,  
824 high helium concentrations (Pinti et al. 2013) in this area may provide indications that a  
825 preferential migration pathway is present in the region, which would allow deep flow  
826 originating from the Appalachians to reach not only the Piedmont (water group A2) but  
827 also the center of the study area (water group M1) along the Richelieu River and around  
828 Monteregian Hills (Figure 4B).]

## 829 **Conclusions**

830 [The multivariate statistical analysis of geochemical parameters from groundwater  
831 samples in the Montérégie Est study area helped define water groups and understand  
832 mechanisms controlling groundwater geochemistry. The identification of four end-  
833 members (two recharge waters, A1 and LL, a brackish Champlain Sea water, CS, and a  
834 geochemical evolution end-member, M1), the aquifer confinement levels and the limit of  
835 the Champlain Sea paleo-environment appear to be the main elements controlling  
836 groundwater geochemical evolution. Even if only a few geochemical mechanisms were  
837 identified and discussed, it was demonstrated that ionic exchange and mixing have a  
838 dominant influence on the overall groundwater composition. Isotopic data were useful to  
839 support hydrogeochemical hypothesis. In particular, indications of residence times from  
840 radiocarbon and tritium confirmed the long residence time of water groups having  
841 indications of geochemical evolution and further supported their relationships.

842 This hydrogeochemical investigation significantly contributed to the understanding of the  
843 regional flow system. The most important contributions that can be attributed to the

844 interpretation of the geochemical results and that would likely have been missed solely  
845 based on physical hydrogeological data, are the following:

- 846 • Identification of the areas of aquifer recharge, which are characterized by young  
847 (high tritium and modern  $^{14}\text{C}$ ) water with relatively low pH and with a composition  
848 controlled by carbonate dissolution ( $\text{Ca-HCO}_3$  water);
- 849 • Delineation of a brackish (non-potable) water zone corresponding to a remnant of  
850 Champlain Sea water that had invaded the rock aquifer. This zone is now under  
851 fully confined conditions and without significant groundwater flow. The  $^{14}\text{C}$  age of  
852 this water corresponds to the Champlain Sea period;
- 853 • Identification of a potentially regional freshwater flow path, originating from the  
854 Appalachian Uplands and emerging into the Piedmont and locally in the Lowlands  
855 (around Monteregeian Hills), which would be responsible for the freshening  
856 mechanism. The geochemical data thus support the occurrence of Tothian nested  
857 flow systems of local, intermediate and regional scales;
- 858 • Evidences that the Piedmont is not a preferential recharge area as presumed initially  
859 at the onset of the project, but rather a regional discharge area for relatively deep  
860 Appalachian groundwater flow with long residence time, which emerges at the  
861 Appalachian's western edge, in the vicinity of the thrust fault zone;
- 862 • Development of a conceptual model of the groundwater flow system integrating the  
863 geochemical interpretation, which gave rise to a major revision of the original  
864 model, and significantly improved our understanding of the regional aquifer  
865 dynamics.

866 ]

## 867 **Acknowledgements**

868 [This study was supported by the regional groundwater resources assessment program  
869 (*Programme d'acquisition de connaissances sur les eaux souterraines*, PACES) of the

870 Quebec Environment Ministry (*Ministère du Développement durable, de*  
871 *l'Environnement et de la Lutte contre les Changements climatiques*, MDDELCC) as well  
872 as the Groundwater Mapping Program of the Geological Survey of Canada. Numerous  
873 regional partners also supported the study through in-kind as well as monetary  
874 contributions, notably the Conférence régionale des élus (CRÉ) de la Montérégie Est.  
875 Authors would also like to acknowledge well owners who allowed the sampling of  
876 groundwater. Finally, we want to thank two anonymous reviewers who made  
877 constructive comments that helped improve the paper significantly.]

## 878 **References**

- 879 [Appelo, C.A.J., Postma, D., 2005. *Geochemistry, groundwater and pollution*. CRC  
880 Press, Boca Raton (FL), USA, 649 pp.
- 881 Beaudry, C., 2013. *Hydrogéochimie de l'aquifère rocheux régional en Montérégie est,*  
882 *Québec* [In French and English]. M.Sc. thesis, INRS, Centre Eau Terre  
883 Environnement, Québec, Canada, 196 pp. <http://espace.inrs.ca/1363/> (Accessed  
884 March, 2018)
- 885 Beaudry, C., Malet, X., Lefebvre, R., Rivard, C., 2011. *Délimitation des eaux*  
886 *souterraines saumâtres en Montérégie Est, Québec, Canada* [In French]. Geological  
887 Survey of Canada, Open File Report 6970, August 2011, 26 pp., doi: 10.4095/289123.
- 888 Blanchette, D., Lefebvre, R., Nastev, M., Cloutier, V., 2010. *Groundwater quality,*  
889 *geochemical processes and groundwater evolution in the Chateauguay River*  
890 *watershed, Quebec, Canada. Canadian Water Resources Journal*, 35(4), 503-526,  
891 doi: 10.4296/cwrj3504503.
- 892 Brisebois, D., Nadeau, J., 2003. *Géologie de la Gaspésie et du Bas-Saint-Laurent* [In  
893 French]. Ministère des Ressources Naturelles, de la Faune et des Parcs, Québec,  
894 Report DV 2003-08, Map scale 1/250 000.
- 895 Carrier, M.-A., Lefebvre, R., Rivard, C., Parent, M., Ballard, J.-M., Benoit, N.,  
896 Vigneault, H., Beaudry, C., Malet, X., Laurencelle, M., Gosselin, J.-S., Ladevèze,

- 897 P., Thériault, R., Beaudin, I., Michaud, A., Pugin, A., Morin, R., Crow, H.,  
898 Gloaguen, E., Bleser, J., Martin, A., Lavoie, D., 2013. Portrait des ressources en  
899 eau souterraine en Montérégie Est, Québec, Canada [In French]. INRS Report  
900 INRS R-1433, June 2013, 318 pp., ISBN: 978-2-89146-764-3.  
901 <http://espace.inrs.ca/1639/> (Accessed March, 2018)
- 902 Clark, T.H., Globensky, Y., Hofmann, H., 1979. Stratigraphie Paléozoïque des Basses-  
903 terres du Saint-Laurent du Québec [In French]. Geological Association of Canada,  
904 Field Trip Guidebook, Edited by Université Laval, Ste-Foy, Québec.
- 905 Clark, I., 2015. Groundwater Geochemistry and Isotopes. CRC Press, Taylor & Francis  
906 Group, Boca Raton, FL, USA, 438 pp.
- 907 Clark, I.D., Fritz, P., 1997. Environmental Isotopes in Hydrogeology. CRC Press, Boca  
908 Raton, FL, USA, 328 pp.
- 909 Cloutier, V., Lefebvre, R., Savard, M., Bourque, É., Therrien, R., 2006.  
910 Hydrogeochemistry and groundwater origin of the Basses-Laurentides sedimentary  
911 rock aquifer system, St. Lawrence Lowlands, Québec, Canada. *Hydrogeology*  
912 *Journal*, 14 (4), 573-590.
- 913 Cloutier, V., Lefebvre, R., Therrien, R., Savard, M., 2008. Multivariate statistical analysis  
914 of geochemical data as indicative of the hydrogeochemical evolution of  
915 groundwater in a sedimentary rock aquifer system. *Journal of Hydrology*, 353 (3-  
916 4), 294-313.
- 917 Cloutier, V., Lefebvre, R., Savard, M.M., Therrien, R., 2010. Desalination of a  
918 sedimentary rock aquifer system invaded by Pleistocene Champlain Sea water and  
919 processes controlling groundwater geochemistry. *Environmental Earth Sciences*,  
920 59(5): 977-994.
- 921 Croteau, A., Nastev, M., Lefebvre, R., 2010. Groundwater recharge assessment in the  
922 Chateauguay River watershed. *Canadian Water Resources Journal*, 35(4), 451-468,  
923 doi: 10.4296/cwrj3504451.

- 924 Davis, J.C., 1986. *Statistics and Data Analysis in Geology*. John Wiley & Sons Inc., New  
925 York.
- 926 Feininger, T., Goodacre, A.K., 1995. The eight classical Montereian hills at depth and  
927 the mechanism of their intrusion. *Canadian Journal of Earth Sciences*, 32(9): 1350-  
928 1364.
- 929 Gaucher, E., 1984. *Compilation de la géologie du Quaternaire - Région des Appalaches*.  
930 Ministère de l'Énergie et des Ressources du Québec, Report DV 84-10, 89 maps  
931 (scale 1/50 000).
- 932 Gibbs, R.J., 1970. Mechanisms controlling world water chemistry. *Science*, 170(3962):  
933 1088-1090.
- 934 Globensky, Y., 1985. *Géologie des Basses-terres du Saint-Laurent* [In French].  
935 Gouvernement du Québec, Ministère de l'Énergie et des Ressources, Direction  
936 générale de l'Exploration géologique et minérale (Ed.), Map no. 1999 of Report  
937 MM 85-02.
- 938 Gouvernement du Québec, 2012. *Règlement sur la qualité de l'eau potable c.Q-2, r.40* [In  
939 French]. Ministère du Développement durable, de la Faune et des Parcs, (Ed.).
- 940 Güler, C., Thyne, G., McCray, J., Turner, K., 2002. Evaluation of graphical and  
941 multivariate statistical methods for classification of water chemistry data.  
942 *Hydrogeology Journal*, 10(4): 455-474.
- 943 Han, L.F., Plummer, L.N., 2016. A review of single-sample-based models and other  
944 approaches for radiocarbon dating of dissolved inorganic carbon in groundwater.  
945 *Earth-Science Reviews* 152 (2016) 119–142, doi: 10.1016/j.earscirev.2015.11.004.
- 946 Han, L.F., Plummer, L.N., Aggarwal, P., 2012. A graphical method to evaluate  
947 predominant geochemical processes occurring in groundwater systems for  
948 radiocarbon dating. *Chemical Geology* 318–319 (2012) 88–112,  
949 doi:10.1016/j.chemgeo.2012.05.004.

- 950 Hem, J.D., 1985. Study and interpretation of the chemical characteristics of natural water.  
951 U.S. Geological Survey, Water Supply Paper 2254, Alexandria, VA, 263 pp.
- 952 Hounslow, A.W., 1995. Water Quality Data: Analysis and Interpretation. Lewis  
953 Publisher, Boca Raton, Florida, USA, 397 pp.
- 954 Jackson, R.E., Heagle, D.J., 2016. Sampling domestic/farm wells for baseline  
955 groundwater quality and fugitive gas. *Hydrogeology Journal*, 24: 269–72.
- 956 Janos, D., 2017. Regional groundwater flow dynamics and residence times in Chaudière-  
957 Appalaches, Québec, Canada: insights from numerical simulations. M.Sc. thesis,  
958 Laval University, Quebec City, Canada, 103 pp.
- 959 Laurencelle, 2018. Propriétés hydrauliques et processus d'invasion par la Mer de  
960 Champlain du système aquifère rocheux fracturé régional de la Montérégie Est,  
961 Québec, Canada. Ph.D. thesis, INRS, Centre Eau Terre Environnement,  
962 <http://ete.inrs.ca/ete/publications/theses-memoires#L>
- 963 Laurencelle, M., Lefebvre, R., Rivard, C., Parent, M., Ladevèze, P., Benoit, N., Carrier,  
964 M.-A., 2013. Modeling the evolution of the regional fractured-rock aquifer system  
965 in the Northern Lake Champlain watershed following last deglaciation.  
966 *GéoMontréal2013, 66<sup>th</sup> Canadian Geotechnical Conference and the 11<sup>th</sup> Joint*  
967 *CGS/IAH-CNC Groundwater Conference*, Montreal, Quebec, Canada, Sept. 29 to  
968 Oct. 3, 2013.
- 969 Lefebvre, R., Rivard, C., Carrier, M.A., Gloaguen, E., Parent, M., Pugin, A., Pullan, S.,  
970 Benoit, N., Beaudry, C., Ballard, J.M., Chasseriau, P., Morin, R.H., 2011.  
971 Integrated regional characterization of the Montérégie Est aquifer system, Quebec,  
972 Canada. *Geohydro2011*, Joint IAH-CNC, CANQUA and AHQ conference, Quebec  
973 City, Canada, August 28-31, 2011, 8 p.
- 974 McCormack, R., 1980. Étude hydrogéologique du bassin versant de la Richelieu [In  
975 French]. Service des eaux souterraines, Direction générale des inventaires et de la  
976 recherche, Ministère de l'Environnement, Gouvernement du Québec, Québec, 47 pp.

- 977 McIntosh, J.C., S.E. Grasby, S.M. Hamilton, et S.G. Osborn, 2014. Origin, distribution  
978 and hydrogeochemical controls on methane occurrences in shallow aquifers,  
979 southwestern Ontario, Canada. *Applied Geochemistry*, 50: 37-52.
- 980 Ministère du Développement durable, de l'Environnement et de la Lutte contre les  
981 changements climatiques (MDDELCC), 2017. Programme de connaissances sur les  
982 eaux souterraines du Québec [In French]. Web site,  
983 [http://www.mddelcc.gouv.qc.ca/eau/souterraines/programmes/acquisition-  
connaissance.htm](http://www.mddelcc.gouv.qc.ca/eau/souterraines/programmes/acquisition-<br/>984 connaissance.htm) (Accessed March, 2018).
- 985 Montcoudiol, N., Molson, J., Lemieux, J.M., Cloutier, V., 2015. A conceptual model for  
986 groundwater flow and geochemical evolution in the southern Outaouais Region,  
987 Québec, Canada. *Applied Geochemistry*, 58, 62-77, doi:  
988 10.1016/j.apgeochem.2015.03.007.
- 989 Occhietti, S., Richard, P.J., 2003. Effet réservoir sur les âges  $^{14}\text{C}$  de la Mer de Champlain  
990 à la transition Pléistocène-Holocène : révision de la chronologie de la déglaciation  
991 au Québec méridional. *Géographie physique et Quaternaire*, 57 (2-3), 115-138.
- 992 Paradis, D., Tremblay, L., Lefebvre, R., Gloaguen, E., Rivera, A., Parent, M., Ballard,  
993 J.M., Michaud, Y., Brunet, P., 2014. Field characterization and data integration to  
994 define the hydraulic heterogeneity of a shallow granular aquifer at a sub-watershed  
995 scale. *Environmental Earth Sciences*, 72 (5), 1325-1348.
- 996 Palmer, S., Campeau, S., Cloutier, V., Daigneault, R., Larocque, M., Lefebvre, R.,  
997 Lemieux, J.M., Molson, J., Rivard, C., Rouleau, A., Therrien, R., 2011.  
998 Collaborative approaches to groundwater knowledge acquisition in Quebec: Inter-  
999 regional characterization. *Geohydro2011*, Joint IAH-CNC, CANQUA and AHQ  
1000 conference, Quebec City, Canada, August 28-31, 2011, 6 p.
- 1001 Parent, M., Occhietti, S., 1988. Late Wisconsinan Deglaciation and Champlain Sea  
1002 Invasion in the St. Lawrence Valley, Québec. *Géographie physique et quaternaire*,  
1003 42(3): 215-246.

- 1004 Pétré, M.A., Rivera, A., Lefebvre, R., Hendry, M.J., Fohnagy, A.J.B., 2016. A unified  
1005 hydrogeological conceptual model of the Milk River transboundary aquifer,  
1006 traversing Alberta (Canada) and Montana (USA). Online 29 June 2016,  
1007 *Hydrogeology J.*, 24(7), 1847-1871, doi: 10.1007/s10040-016-1433-8.
- 1008 Pinti, D.L., Gélinas, Y., Larocque, M., Barnetche, D., Retailleau, S., Moritz, A., Helie,  
1009 J.F., Lefebvre, R., 2013. Concentrations, sources et mécanismes de migration  
1010 préférentielle des gaz d'origine naturelle (méthane, hélium, radon) dans les eaux  
1011 souterraines des Basses-Terres du Saint-Laurent [In French]. Volet géochimie,  
1012 Étude E3-9, FQRNT ISI n° 171083, UQAM, U. Concordia, INRS, Août 2013, 94  
1013 p. [http://www.bape.gouv.qc.ca/sections/mandats/gaz\\_de\\_schiste-  
1014 enjeux/documents/PR3.6.9.pdf](http://www.bape.gouv.qc.ca/sections/mandats/gaz_de_schiste-enjeux/documents/PR3.6.9.pdf) (Accessed in March, 2018)
- 1015 Plummer, L.N., Glynn, P.D., 2013. Radiocarbon dating in groundwater systems. Chapter  
1016 4, 33-89, In *Dating Old Groundwater: A Guidebook*, IAEA, Vienna, ISBN 978-92-  
1017 0-137210-9.
- 1018 Prichonnet, G., 1984. Dépôts quaternaires de la région de Granby, Québec [In French].  
1019 Commission géologique du Canada (Ed.), Étude 83-30, Ottawa, Canada, 8 pp.
- 1020 Rey, N., Rosa, E., Cloutier, V., Lefebvre, R., 2017. Using water stable isotopes for  
1021 tracing surface and groundwater flow systems in the Barlow-Ojibway Clay Belt,  
1022 Quebec, Canada. Online 11 December 2017, *Canadian Water Resources J.*, 22 pp.,  
1023 doi: 10.1080/07011784.2017.1403960.
- 1024 Sanford, R.F., Pierson, C.T., Crovelli, R.A., 1993. An objective replacement method for  
1025 censored geochemical data. *Mathematical Geology*, 25(1): 59-80.
- 1026 Schroeder, P.R., Aziz, N.M., Lloyd, C.M., Zappi, P.A., 1994. The hydrologic evaluation  
1027 of landfill performance (HELP) model: Engineering documentation for version 3.  
1028 EPA/600/R-94/168b. U.S. Environmental Protection Agency, Office of Research  
1029 and Development, Washington, D.C., 126 pp.

- 1030 Séjourné, S., Lefebvre, R., Malet, X., Lavoie, D., 2013. Synthèse géologique et  
1031 hydrogéologique du Shale d'Utica et des unités sus-jacentes (Lorraine, Queenston  
1032 et dépôts meubles), Basses-Terres du Saint-Laurent, Province de Québec.  
1033 Geological Survey of Canada, Open File 7338, 156 p.
- 1034 Slivitzky, A., Saint-Julien, P., 1987. Compilation géologique de la région de l'Estrie-  
1035 Beauce [In French]. Ministère de l'Énergie et des Ressources, Report MM 85-04,  
1036 Québec, Canada, 48 pp., 1 map (1/ 250 000).
- 1037 StatSoft Inc., 2004. STATISTICA (Data Analysis Software System), Version 6.
- 1038 Tóth, J., 1963. A theoretical analysis of groundwater flow in small drainage basins.  
1039 *Journal of Geophysical Research*, 68(16), 4795–4812, doi:  
1040 10.1029/JZ068i016p04795.
- 1041 Tóth, J., 1999. Groundwater as a geologic agent: An overview of the causes, processes,  
1042 and manifestations. *Hydrogeology Journal*, 7(1), 1–14, doi:  
1043 10.1007/s100400050176.
- 1044 Tremblay, L., Lefebvre, R., Paradis, D., Gloaguen, E., 2014. Conceptual model of  
1045 leachate migration in a granular aquifer derived from the integration of multi-  
1046 source characterization data (St-Lambert, Canada). *Hydrogeology J.*, 22(3), 587-  
1047 608.
- 1048 Valder, J.F., Long, A.J., Davis, A.D., Kenner, S.J., 2012. Multivariate statistical approach  
1049 to estimate mixing proportions for unknown end members. *Journal of Hydrology*,  
1050 460-461: 65-76.
- 1051 Vautour, G., Pinti, D.L., Méjean, P., Saby, M., Meyzonnat, G., Larocque, M., Castro,  
1052 M.C., Hall, C.M., Boucher, C., Roulleau, E., Barbecot, F., Takahata, N., Sanoc, Y.,  
1053 2015.  $^3\text{H}/^3\text{He}$ ,  $^{14}\text{C}$  and (U–Th)/He groundwater ages in the St. Lawrence  
1054 Lowlands, Quebec, Eastern Canada. *Chemical Geology* 413 (2015) 94–106.
- 1055 ]

1056

For Peer Review Only

1057 **Figure Captions**

1058

1059 Figure 1. Montérégie Est location and hydrogeological contexts based on physiography.  
1060 Map also shows topography, main roads, the Champlain Sea maximum marine  
1061 transgression limit (~11 000 years ago) and the trace of the cross-sections shown on the  
1062 3D block diagram of **Figure 2** (dashed red lines).

1063

1064 Figure 2. 3D block diagram of subsurface conditions in Montérégie Est (cross-sections  
1065 locations shown on **Figure 1**). The generally east-west cross-section goes from the  
1066 Lowlands to the Appalachian Uplands and crosses the thrust faults of the Appalachian  
1067 Front. The generally north-south cross-section remains in the Lowlands but crosses a  
1068 Monteregian Hill. Till (green) covers most of the bedrock, with local accumulations of  
1069 fluvio-glacial sediments (orange) or old sediments (brown), and is apparent at surface in  
1070 the Appalachian Piedmont and Uplands. Lacustrine (purple) and marine (light blue) fine  
1071 sediments can form large accumulations in the North Lowlands (more than 30 m thick).

1072

1073 Figure 3. Confinement level of the Montérégie Est fractured rock aquifer system and  
1074 extent of brackish groundwater, to the north of the region.

1075

1076 Figure 4. Results of multivariate statistical analysis of geochemical parameters. A)  
1077 Cluster Analysis tree diagram defining the 8 water groups below a phenon line of 18. B)  
1078 Spatial distribution of the 190 samples with colored areas belonging to a water group. C)  
1079 Values of the 1<sup>st</sup> and 2<sup>nd</sup> components of the Principal Component Analysis for the 190  
1080 samples identified with their water group. The names of water groups were assigned on  
1081 the basis of their spatial distribution (**Figure 4B**) and their geochemical characteristics  
1082 (**Figure 5**): three “Appalachian” groups A1, A2 and A3; a “Lowland” group LL; a

1083 “Champlain Sea” group CS; and three “Mixed” or “Monteregian” groups M1, M2 and  
1084 M3.

1085

1086 Figure 5. Major ions in groundwater. A) Proportions of major ions for each sample,  
1087 associated with its water group (color), represented on a Piper diagram. B) Average ionic  
1088 composition for each water group represented by Stiff diagrams (ions represented and  
1089 concentration scale shown to the left of diagrams). The order of Stiff diagrams is based  
1090 on relations between water groups and geochemical evolution paths that will be discussed  
1091 later.

1092

1093 Figure 6. Geochemical conditions for the water groups found in Montérégie Est. A  
1094 Average  $p_e$  and pH values for the eight water groups. B) Champlain Sea water mixing.  
1095 C) Carbonate dissolution mechanism indicated by a  $\text{Ca}/\text{HCO}_3$  ratio (in mmol/L) of 1:2  
1096 (dashed line). D) Evidence of groundwater freshening due to Na-Ca ion exchange.

1097

1098 Figure 7. Mixing and relations between water groups and groundwater geochemical end-  
1099 members. A) Samples of water groups defined in [Figures 4 and 5](#) according to the 1<sup>st</sup> and  
1100 2<sup>nd</sup> components of the Principal Component Analysis (PCA). B) Relative concentrations  
1101 of major cations (X-axis) and major anions (Y-axis), similar to a Piper plot, supporting  
1102 relations shown on the PCA graph. Inferred geochemical end-members are superposed on  
1103 both graphs: Sea Water, Lowland Recharge, Monteregian Water and Appalachian  
1104 Recharge.

1105

1106 Figure 8. Isotopic composition of groundwater. A) Stable isotopes of groundwater by  
1107 groups compared to the Basses-Laurentides meteoric water line (BLMWL; [Cloutier et al.](#)  
1108 [2006](#)). B) Residence time of water groups indicated by tritium ( $^3\text{H}$  is in tritium units, TU)  
1109 and radiocarbon (non-corrected  $^{14}\text{C}$  ages in years before present, BP). Samples analyzed

1110 for only one of the two parameters are still represented in the left and bottom margins of  
1111 the graph. Ellipses indicate the distribution of samples for water groups.

1112

1113 Figure 9. Geochemical evolution paths and residence time. A) Na/Ca ratio versus  
1114 uncorrected  $^{14}\text{C}$  ages. B) Corrected  $^{14}\text{C}$  age range of water groups (Table 3). Sample  
1115 colors are related to water groups as defined in Figures 4A and 5.

1116

1117 Figure 10. Conceptual model of groundwater geochemical evolution in Montérégie Est.  
1118 Each of the 8 water groups is represented with the direction of evolution (arrows) and the  
1119 main mechanisms involved (mixing, geological influence, ion exchange) and the  
1120 corrected radiocarbon age range (see Table 3).

1121

1122 Figure 11. Geochemical conceptual model represented by a schematic cross-section from  
1123 the Appalachian Uplands to the St. Lawrence River. Water group locations are illustrated  
1124 with associated colors and flow directions are represented by arrows. The limit of the  
1125 former Champlain Sea is indicated by dashed lines on the map and section.

1126

1

2 **Table 1. Loadings of the 16 geochemical parameters for the first 5 components (C1**  
 3 **through C5) of the Principal Component Analysis (bold values indicate dominant**  
 4 **parameters).**

5

Parameters	C1	C2	C3	C4	C5
pH	-0.384	0.535	0.117	<b>0.594</b>	-0.054
pe	0.549	0.044	-0.381	<b>-0.475</b>	-0.156
TDS	<b>-0.899</b>	0.065	-0.332	-0.075	0.110
HCO <sub>3</sub>	<b>-0.834</b>	0.181	-0.015	-0.164	0.172
NH <sub>4</sub>	<b>-0.831</b>	0.145	0.191	-0.069	-0.019
Ba	-0.693	-0.100	<b>0.489</b>	-0.141	-0.199
B	<b>-0.808</b>	0.439	-0.052	-0.020	-0.099
Ca	-0.162	<b>-0.937</b>	-0.058	-0.063	-0.164
Cl	-0.733	0.017	-0.393	-0.167	0.141
Mg	-0.422	<b>-0.802</b>	0.043	-0.015	-0.221
Mn	-0.286	-0.629	0.123	0.250	0.221
K	-0.793	-0.059	-0.006	-0.224	-0.093
Si	-0.182	-0.525	0.290	-0.135	<b>0.665</b>
Na	<b>-0.803</b>	0.4223	-0.268	0.083	0.061
Sr	-0.603	-0.570	0.002	0.158	-0.356
SO <sub>4</sub>	0.0164	-0.545	<b>-0.648</b>	0.365	0.103
% total variance	<b>39.2</b>	<b>22.2</b>	8.1	6.0	5.3

8

9

1

2

3

4

**Table 2. Median values of physico-chemical parameters and component concentrations (mg/L) for the water groups defined in Figure 4 (geochemical data and water group statistics are available in Beaudry 2013).**

Category	Parameter	CS N=3	M3 N=19	M1 N=19	M2 N=14	LL N=46	A2 N=26	A3 N=41	A1 N=22
Physico-chemical	pH	7.59	8.26	<b>8.69</b>	7.805	7.235	7.855	7.83	<u>6.405</u>
	TDS	<b>2961</b>	1340	723	517	673	321	283	<u>168</u>
	D.O.	<u>0.17</u>	0.34	0.32	0.49	0.37	0.525	0.38	<b>5.745</b>
	pe	<u>-0.41</u>	3.15	2.35	2.09	3.29	5.39	3.55	<b>6.49</b>
Major ions	Na	<b>630</b>	380	190	74	34	60.5	9.7	<u>4</u>
	Ca	<b>310</b>	9.2	<u>3.8</u>	30	85.5	12.5	35	28
	Mg	<b>110</b>	11	<u>1.5</u>	17.5	28	4.45	11	4.25
	Cl	<b>340</b>	260	39	25.5	38	14	7.9	<u>6.3</u>
	SO <sub>4</sub>	<b>1500</b>	<u>0.5</u>	13	2.2	66.5	27.5	18	13
	HCO <sub>3</sub>	158.0	<b>642.1</b>	351.5	355.6	329.0	180.4	158.4	<u>89.0</u>
Minor ions	K	<b>23</b>	5.6	1.7	4.95	3.05	0.835	0.8	<u>0.74</u>
	Sr	<b>9.1</b>	0.83	<u>0.19</u>	2.85	1.85	0.905	0.6	0.2
	Fe	<b>1.2</b>	0.14	<u>0.015</u>	0.17	0.36	0.024	0.11	<u>0.015</u>
	F	0.5	<b>1.2</b>	1	0.5	0.1	0.45	0.1	<u>0.05</u>
	CO <sub>3</sub>	0.219	2.665	<b>6.821</b>	0.716	0.190	0.576	0.266	<u>0.009</u>
	N-NO <sub>3</sub>	0.01	0.01	0.01	0.01	0.01	0.01	0.01	<b>0.43</b>
	NH <sub>4</sub>	<b>2.8</b>	1.5	0.47	0.96	0.26	0.045	0.06	<u>0.03</u>
Traces	Ba	0.016	0.6	0.074	<b>1.15</b>	0.15	0.033	0.074	<u>0.0115</u>
	B	<b>1.2</b>	0.51	0.36	0.225	0.0505	0.038	0.009	<u>0.0025</u>
	Br	<b>0.5</b>	<b>0.5</b>	0.05	0.05	0.05	0.05	0.05	0.05
	Mn	<b>0.36</b>	0.011	0.0055	0.023	0.0785	0.0265	0.071	<u>0.00225</u>

5

6

7

Notes: N is the number of available measurements for the water group. TDS is Total Dissolved Solids. D.O. is Dissolved Oxygen (mg/L). N-NO<sub>3</sub> also includes N-NO<sub>2</sub>.

8

1

2 **Table 3. Ranges of tritium ( $^3\text{H}$ ), uncorrected (lab.) and corrected  $^{14}\text{C}$  ages for the**  
 3 **water groups.**

Water Group	$^3\text{H}$ range <sup>1</sup> (TU)	$^{14}\text{C}$ values <sup>2</sup> (Analyses)	Range of Lab. Age (ky BP)	Rounded Min. Age (ky BP)	Middle of Range (ky BP)	Rounded Max. Age (ky BP)
<b>CS</b>	6.6 (1)	2 (3)	14.2-14.8	13.9	13.9	13.9
<b>M3</b>	0.0 (3)	4 (4)	3.8-16.6	3.6	8.8	14.0
<b>M1</b>	3.2-4.9 (3)	4 (4)	7.2-12.5	4.3	5.5	6.7
<b>M2</b>	1.0-9.6 (3)	3 (5)	2.3-6.1	Modern	1.95	3.9
<b>LL</b>	10.4-12.6 (6)	2 (4)	0.06-5.2	Modern	0.75	1.5
<b>A2</b>	0.4-4.2 (8)	7 (7)	6.2-16.0	3.0	7.5	12.0
<b>A3</b>	6.3-9.7 (11)	6 (7)	3.3-11.8	3.0	6.0	9.0
<b>A1</b>	13.2-14.5 (4)	0 (4)	0.0-3.2	Modern	Modern	Modern

4

5

6

7

8

1: 25<sup>th</sup> to 75<sup>th</sup> percentiles of the number of analyses in bracket. 2: The number of quantitatively interpreted  $^{14}\text{C}$  age values among the number of available analyses. Analyses that could not be interpreted were either modern groundwater or had a  $\log(\text{pCO}_2)$  value exceeding -2.0 indicative of an open  $\text{CO}_2$  system (Clark 2015).

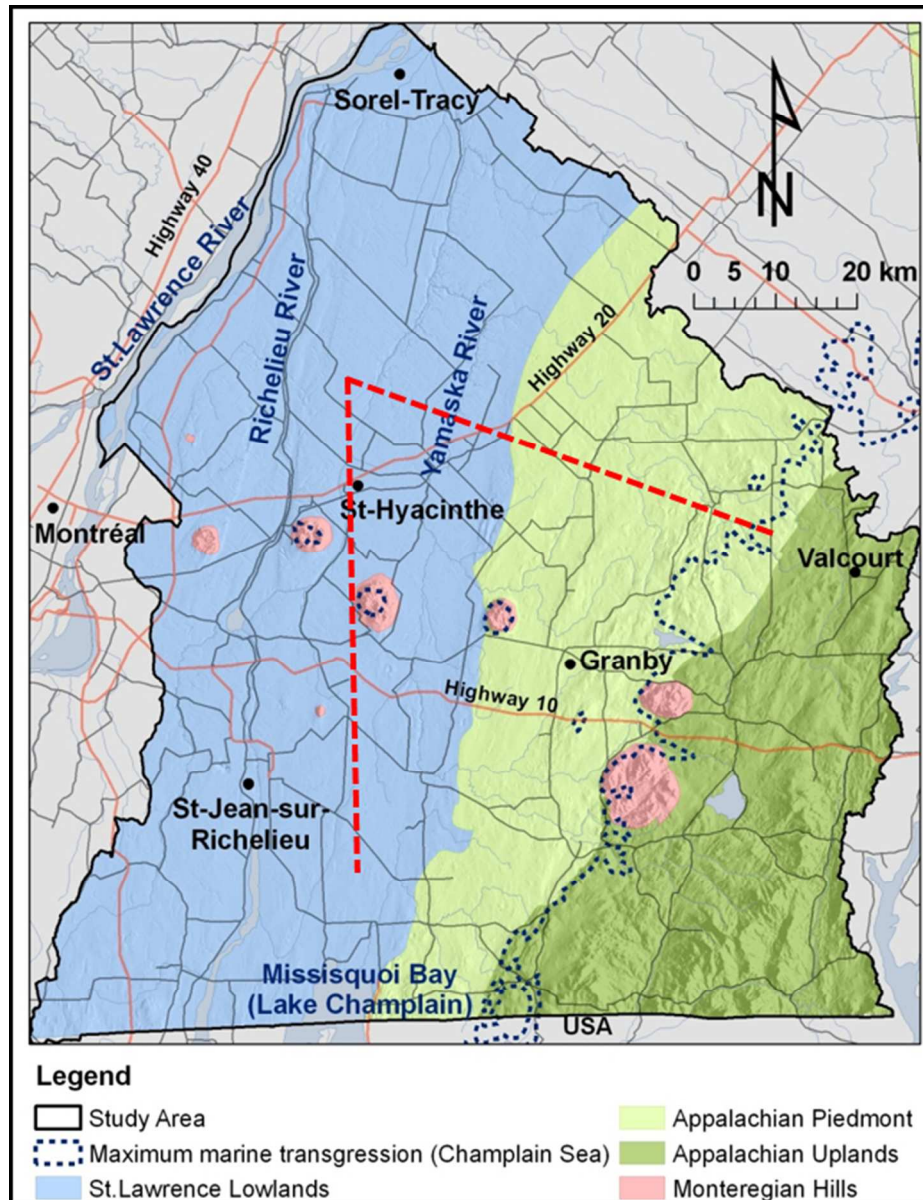


Figure 1. Montérégie Est location and hydrogeological contexts based on physiography. Map also shows topography, main roads, the Champlain Sea maximum marine transgression limit (~11 000 years ago) and the trace of the cross-sections shown on the 3D block diagram of Figure 2 (dashed red lines).

109x141mm (150 x 150 DPI)

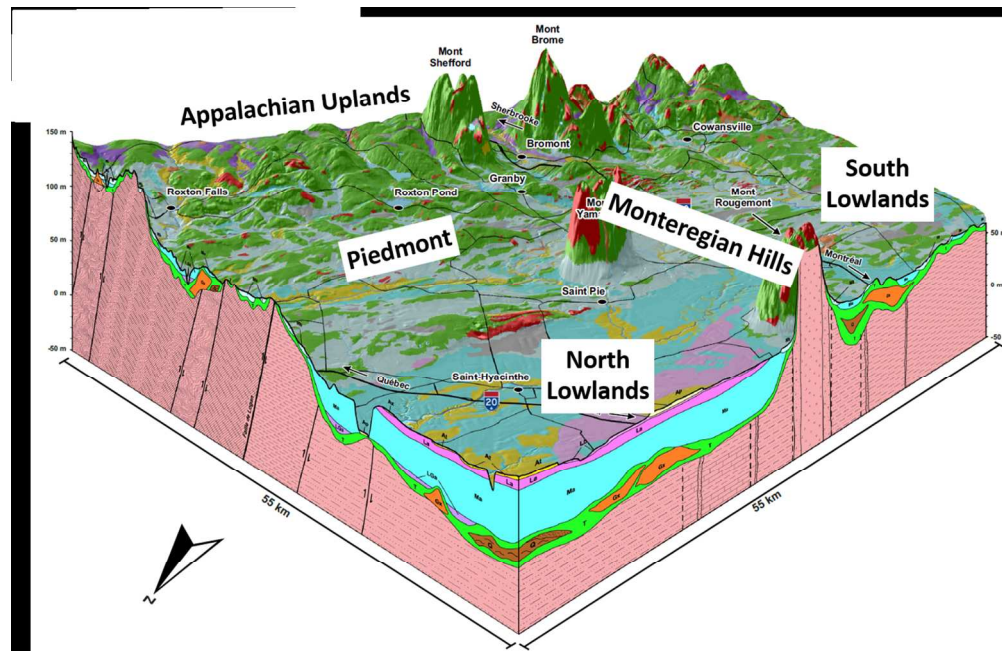


Figure 2. 3D block diagram of subsurface conditions in Montérégie Est (cross-sections locations shown on Figure 1). The generally east-west cross-section goes from the Lowlands to the Appalachian Uplands and crosses the thrust faults of the Appalachian Front. The generally north-south cross-section remains in the Lowlands but crosses a Monteregian Hill. Till (green) covers most of the bedrock, with local accumulations of fluvio-glacial sediments (orange) or old sediments (brown), and is apparent at surface in the Appalachian Piedmont and Uplands. Lacustrine (purple) and marine (light blue) fine sediments can form large accumulations in the North Lowlands (more than 30 m thick).

240x155mm (150 x 150 DPI)

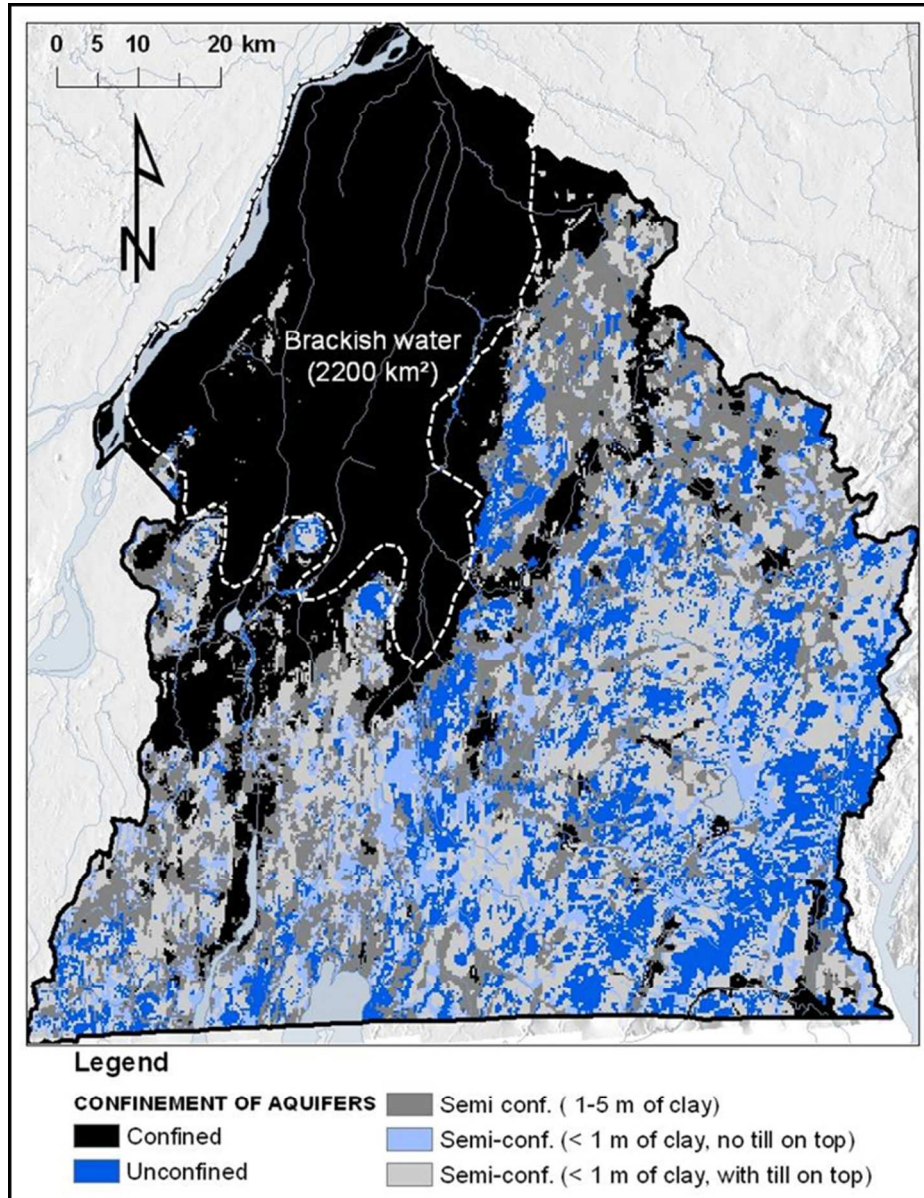


Figure 3. Confinement level of the Montérégie Est fractured rock aquifer system and extent of brackish groundwater, to the north of the region.

126x163mm (150 x 150 DPI)

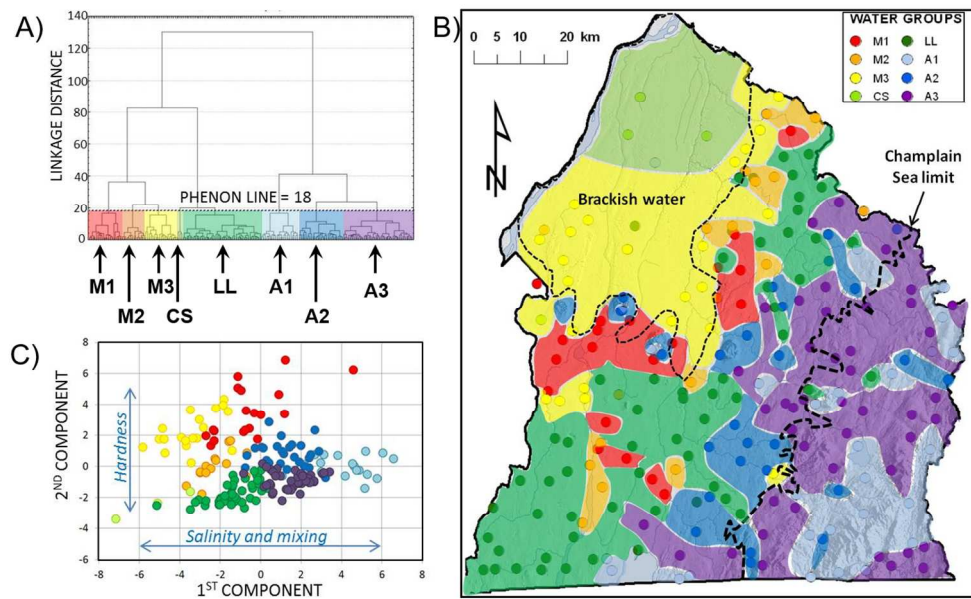


Figure 4. Results of multivariate statistical analysis of geochemical parameters. A) Cluster Analysis tree diagram defining the 8 water groups below a phenon line of 18. B) Spatial distribution of the 190 samples with colored areas belonging to a water group. C) Values of the 1st and 2nd components of the Principal Component Analysis for the 190 samples identified with their water group. The names of water groups were assigned on the basis of their spatial distribution (Figure 4B) and their geochemical characteristics (Figure 5): three "Appalachian" groups A1, A2 and A3; a "Lowland" group LL; a "Champlain Sea" group CS; and three "Mixed" or "Monteregian" groups M1, M2 and M3.

251x154mm (150 x 150 DPI)

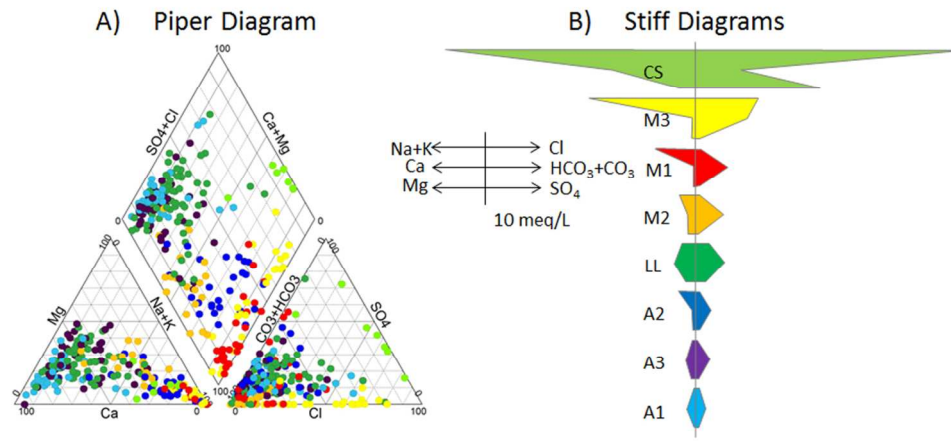


Figure 5. Major ions in groundwater. A) Proportions of major ions for each sample, associated with its water group (color), represented on a Piper diagram. B) Average ionic composition for each water group represented by Stiff diagrams (ions represented and concentration scale shown to the left of diagrams). The order of Stiff diagrams is based on relations between water groups and geochemical evolution paths that will be discussed later.

222x100mm (150 x 150 DPI)

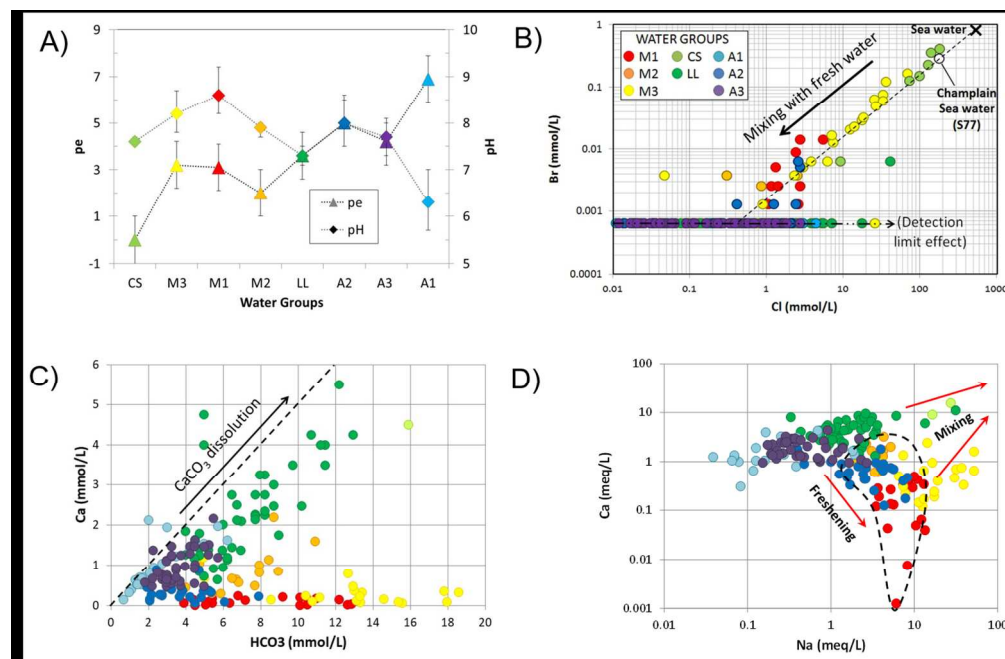


Figure 6. Geochemical conditions for the water groups found in Montérégie Est. A Average pe and pH values for the eight water groups. B) Champlain Sea water mixing. C) Carbonate dissolution mechanism indicated by a Ca/HCO<sub>3</sub> ratio (in mmol/L) of 1:2 (dashed line). D) Evidence of groundwater freshening due to Na-Ca ion exchange.

247x160mm (150 x 150 DPI)

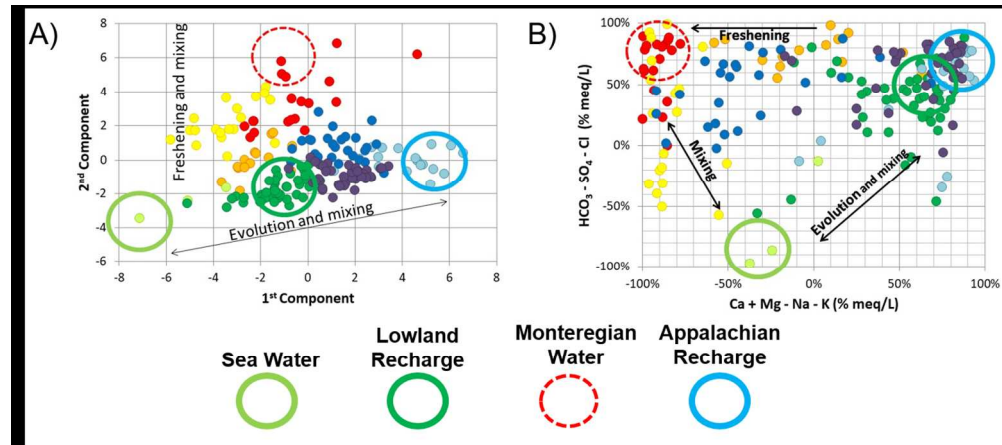


Figure 7. Mixing and relations between water groups and groundwater geochemical end-members. A) Samples of water groups defined in Figures 4 and 5 according to the 1st and 2nd components of the Principal Component Analysis (PCA). B) Relative concentrations of major cations (X-axis) and major anions (Y-axis), similar to a Piper plot, supporting relations shown on the PCA graph. Inferred geochemical end-members are superposed on both graphs: Sea Water, Lowland Recharge, Monteregian Water and Appalachian Recharge.

240x105mm (150 x 150 DPI)

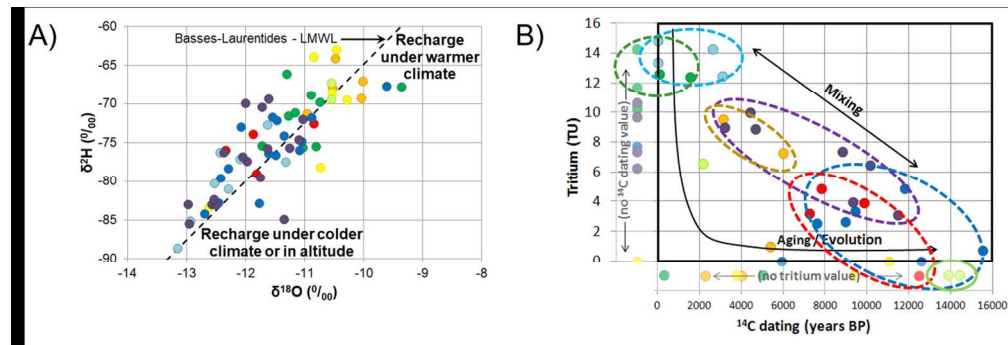


Figure 8. Isotopic composition of groundwater. A) Stable isotopes of groundwater by groups compared to the Bases-Laurentides meteoric water line (BLMWL; Cloutier et al. 2006). B) Residence time of water groups indicated by tritium ( $^3\text{H}$  is in tritium units, TU) and radiocarbon (non-corrected  $^{14}\text{C}$  ages in years before present, BP). Samples analyzed for only one of the two parameters are still represented in the left and bottom margins of the graph. Ellipses indicate the distribution of samples for water groups.

246x83mm (150 x 150 DPI)

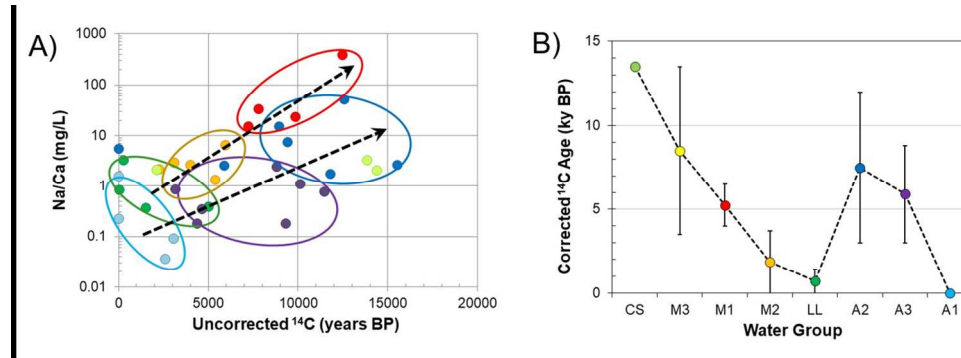


Figure 9. Geochemical evolution paths and residence time. A) Na/Ca ratio versus uncorrected  $^{14}\text{C}$  ages. B) Corrected  $^{14}\text{C}$  age range of water groups (Table 3). Sample colors are related to water groups as defined in Figures 4A and 5.

245x86mm (150 x 150 DPI)

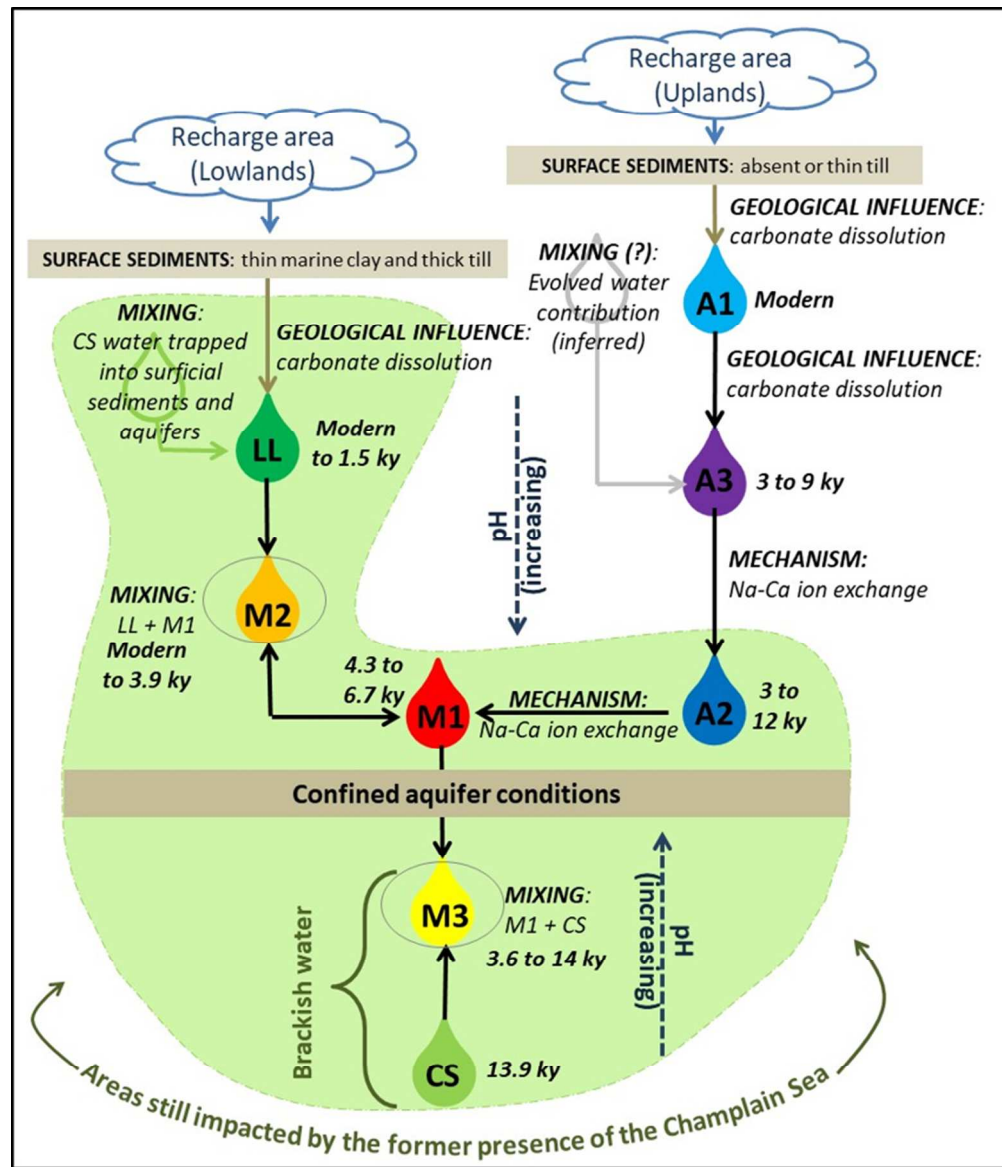


Figure 10. Conceptual model of groundwater geochemical evolution in Montérégie Est. Each of the 8 water groups is represented with the direction of evolution (arrows) and the main mechanisms involved (mixing, geological influence, ion exchange) and the corrected radiocarbon age range (see Table 3).

143x167mm (150 x 150 DPI)

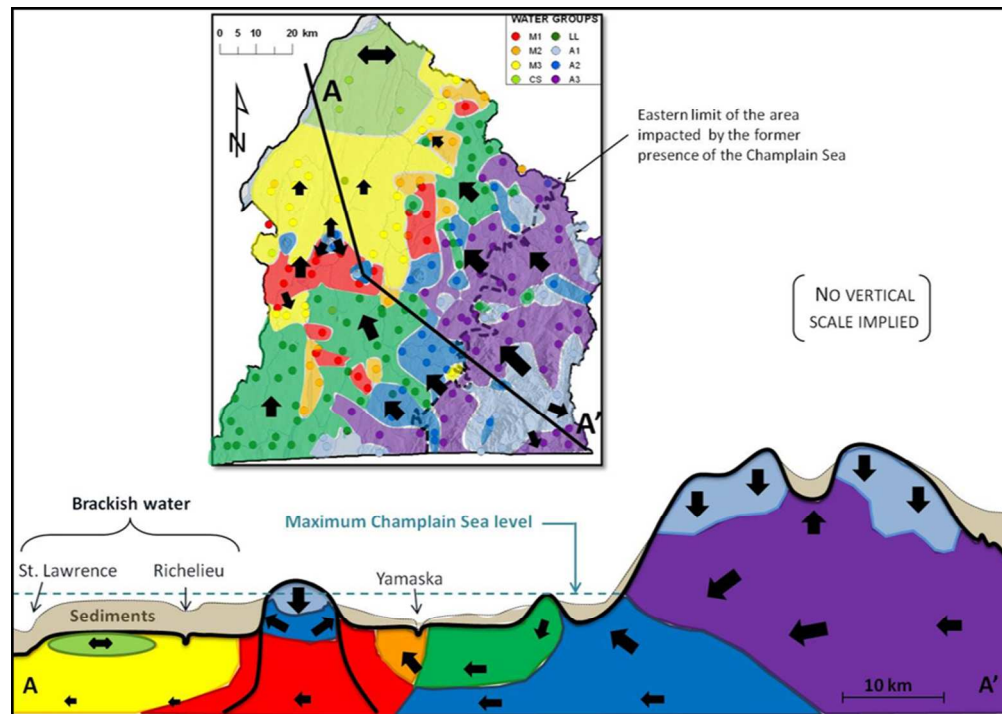


Figure 11. Geochemical conceptual model represented by a schematic cross-section from the Appalachian Uplands to the St. Lawrence River. Water group locations are illustrated with associated colors and flow directions are represented by arrows. The limit of the former Champlain Sea is indicated by dashed lines on the map and section.

166x118mm (150 x 150 DPI)